Contents

1 Bayesian model fitting applied to flow cytometry data

1.1 Introduction

In this chapter I aim to fit the toggle switch model to experimental data. This chapter is organised as follows: In the first section I provide an overview of the framework developed to fit models to flow cytometry data (ABC-Flow). In the subsequent section I test ABC-Flow on simulated flow cytometry data. Next I use flow cytometry to study the toggle switch experimentally and examine the concentrations of the inducers and the time needed to flip the switch. Finally, I use ABC-Flow to fit a computational model to the experimental data acquired.

1.2 Contributions to this Chapter

The R code used to pre-process the flow cytometry obtained was provided by Alex J. Fedorec. The R code to fit the Hill function to the flow cytometry concentration assays was adapted from code provided by David T. Gonzales.

1.3 Flow cytometry and model fitting

Computational modelling is well known to aid the understanding of complex systems by fitting experimental data and providing further insights and testable predictions. Experimental data is used to fit the model parameters and then the model can provide further understanding of the system and aid in the design of further experiments. Flow cytometry is used in synthetic biology for BioBrick characterisation (Kelly et al. 2009), enzyme screening (Choi et al. 2014) and industrial bioprocesses (Díaz et al. 2010) among others.

Flow cytometry data presents a challenge to computational modelling as the fluorescence intensity per cell is measured rather than number of proteins. The problem with measuring fluorescence intensity is that it is a relative and not an absolute measurement like the number or concentration of proteins in a system, which would increase the predictive power of computational models (Bower, McClintock, & Fong 2010; Cooling et al. 2010), but this type of biological data cannot be directly measured (Kelwick et al. 2014). The fluorescence intensity values can vary between experiments due to instrument settings so they can only be used in relative terms within the same experiment. Standardization of experimental methods in flow cytometry has aided the effort to reduce variability due to experimental setup (Kelly et al. 2009), but the successful conversion of fluorescence intensity to an absolute measurement of protein $cell^{-1}$ s^{-1} has yet to be made successfully.

Another approach to the problem is converting the model output of GFP $cell^{-1}$ s^{-1} to relative fluorescence intensity. This approach was first developed by Lillacci & Khammash (2013). The converted model output can then be compared to the data output from the flow cytometer. The fluorescent intensity measurements acquired via flow cytometry are treated as a sample from distribution of the fluorescence present in the cell (Lillacci & Khammash 2013). This means that the flow cytometry fluorescence distribution at each time point can be compared to the model fluorescence distribution. Here I expand the method developed by Lillacci & Khammash (2013) in order to be able to apply it to flow cytometry data including two fluorescent proteins simultaneously. This new framework, ABC-Flow, can be used to fit stochastic models to flow cytometry data involving two species, like the genetic toggle switch.

1.4 ABC-Flow algorithm development

The algorithm of ABC-Flow is based on the same ABC algorithm as ABC-SysBio and Stability Finder described in Sections (XXX), adapted to be used for flow cytometry data. The algorithm of ABC-Flow is outlined in Algorithm 1. The modified modules of the ABC algorithm are outlined in the sections that follow.

The user provides an SBML model file and an input file to specify the information needed to run ABC-Flow, such as the epsilon schedule and the priors to the parameters. The user must also provide a data file containing the flow cytometry data to which the model will be fitted. The data files used here were generated from .fcs files, which is the standard output of flow cytometers, using the R bioconductor

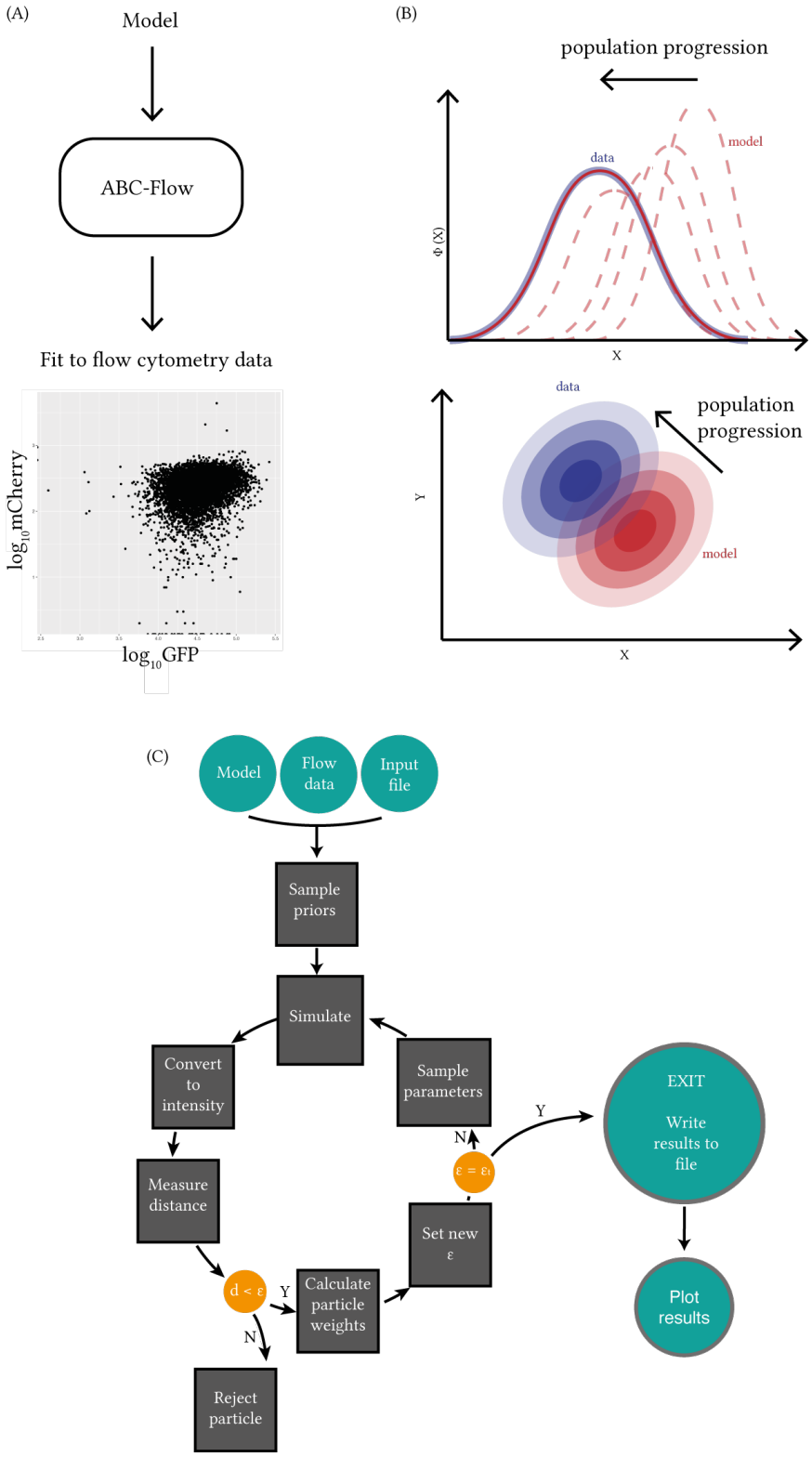

Figure 1.1 Overview of ABC-Flow. (A) ABC-Flow is used to fit models to experimental flow cytometry data. (B) The algorithm can be applied to 1D and 2D flow data. (C) ABC-Flow uses Approximate Bayesian Computation.

packages flowCore (Ellis et al. 2016b). All models are simulated stochastically using the Gillespie algorithm (Gillespie 1977). ABC-Flow simulations are implemented on GPUs. ABC-Flow is available as a Python package, and can be downloaded from https://github.com/ucl-cssb/ABC-Flow.git.

Algorithm 1 ABC-Flow

1: Initialise ϵ
2: population p $\leftarrow 1$
3: **if** p $= 1$ **then**
4: Sample particles (θ) from priors
5: **else**
6: Sample particles from previous population
7: Perturb each particle by $\pm$ half the range of the previous population (j) to obtain new perturbed population (i).
8: **end if**
9: Simulate model using the Gillespie algorithm.
10: Convert signal to intensity:
11: **for** each particle **do**
12: **for** each beta **do**
13: **for** each timepoint **do**
14: **for** each fluorescent protein **do**
15: Intensity = $\mathrm{N}\left(\text{signal}\times\mu, \sqrt{(signal \times \sigma^2)}\right)$
16: **end for**
17: **end for**
18: **end for**
19: **end for**
20: Measure distance to data
21: Reject particles if d $> \epsilon$.
22: Calculate weight for each accepted θ
23: $w_t^{(i)} = \begin{cases} 1, & \text{if } p = 0 \\ \frac{\pi(\theta_t^{(i)})}{\sum_{j=1}^{N} w_{t-1}^{(j)} K_t(\theta_{t-1}^{(j)}, \theta_t^{(i)})}, & \text{if } p \geq 0. \end{cases}$
24: Normalise weights
25: Repeat steps 3 - 15 until $\epsilon \leq \epsilon_T$

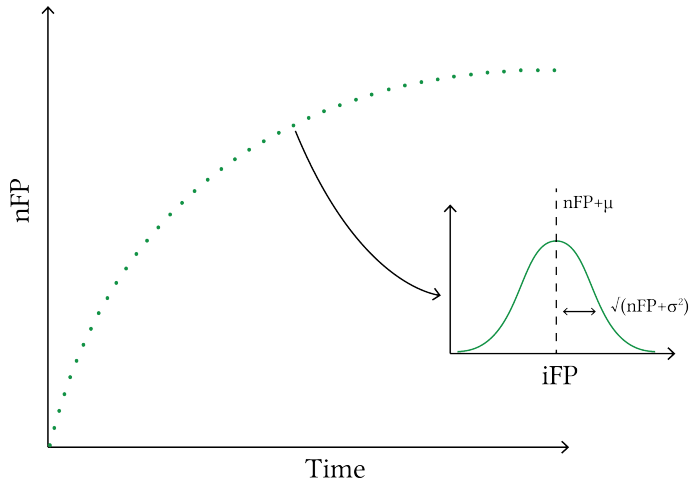

Figure 1.2 Converting the number of fluorescent proteins to the intensity (iFP) is done by drawing from a normal distribution, as shown in Equation 1.1.

1.4.1 Intensity calculation

The units of the result of the stochastic simulations is in the form of number of fluorescent proteins. On the other hand, flow cytometry data units are in the form of fluorescence intensity. For ABC-Flow, the simulation results are converted to intensity in order to be able to compare the data to the simulations. In order to do this two additional parameters are defined, intensity μ and intensity σ, for each fluorescent protein used. To convert the number of fluorescent proteins to intensity, random samples are drawn from a normal distribution:

$$X \sim N\Big(nFP \times \mu, \sqrt{(nFP \times \sigma^2)}\Big), \tag{1.1}$$

where nFP is the number of fluorescent proteins.

These parameters are fitted to the data along with the model parameters.

1.4.2 Distance Calculations

In order to compare the flow cytometry data to the model generated data, I had to develop a distance measure. This distance measure should be able to determine whether two datasets are sufficiently close to each other to be able to be assume that they have been drawn from the same distribution. The measure should also give an estimate of how different the two data sets are, and thus get increasingly

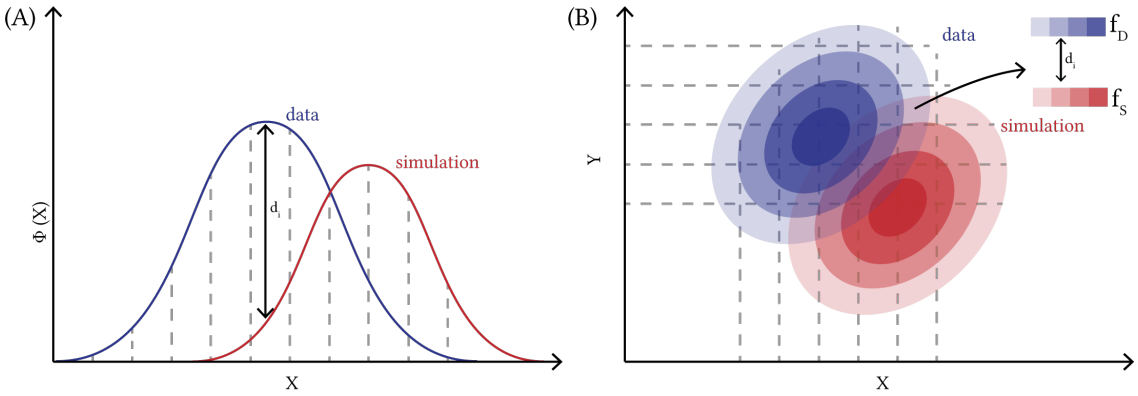

Figure 1.3 Calculating the distance between two distributions in (A) 1D and (B) 2D.

larger as two data sets are drawn from increasingly different distributions. Finally the distance measure should be applicable to one and two dimensional distributions, and be comparable between the two.

1.4.2.1 Kernel distance

In order to measure the distance between the flow cytometry data and the fitted model, the algorithm outlined in Algorithm 2 was developed. The algorithm consists of defining a grid from the minimum to the maximum value of the data. A gaussian kernel was then fit to the flow and simulated data. The distance between the two kernels is given by:

$$d = \sum_{i=xmin}^{xmax} (fD_i - fS_i)^2,$$

where fD_i is the kernel of the flow data at each value of x and fS_i the kernel of the simulaed data. An illustration of the distance calculation is shown in Figure 1.3.

Algorithm 2 Distance calculation

1: Grid ← min(data):max(data):ngrid
2: kD = kernel density estimation(data)
3: kS = kernel density estimation(simulations)
4: fD = kD(xx)
5: fS = kS(xx)
6: $epsilon = \sum((fD - fS)^2)$

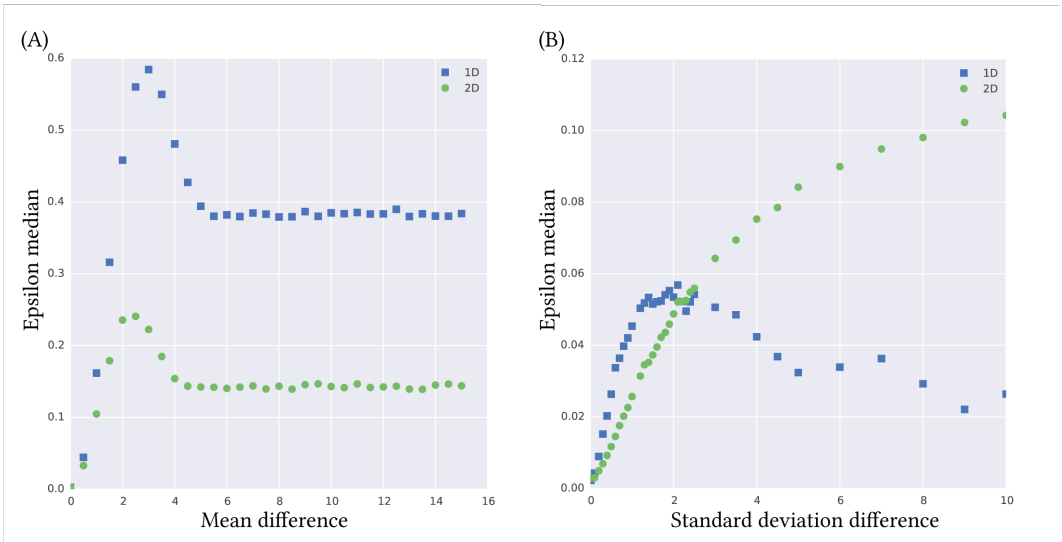

Figure 1.4 (A) The range by which epsilon varies as the difference between the mean of the distributions increases. (B) The median of the epsilon distributions varies by a small amount with increasing difference in the standard deviation of the distributions.

Prior to incorporating this distance calculation in ABC-FLow, it was tested to determine whether it is an appropriate distance to use when comparing distributions. This was done by drawing samples form two uniform distributions with varying mean and standard deviation. Algorithm 2 was then used to calculate the distance between the different distributions.

First, Algorithm 2 was tested by drawing samples from two distributions with an increasingly different mean. This is done to determine the dynamical range of the distance calculation.

From Figure 1.4 we see that the epsilon value does not increase linearly with increasing mean difference of the two distributions. As the difference between the means increases, the epsilon value reaches a peak when the difference is at 3. From that point, as the mean difference increases, epsilon values decrease until they reach a plateau at epsilon = 0.38 in the 1D case and epsilon = 0.14 in the 2D case. Next, I test the distance calculation by comparing bimodal distributions. Two bimodal distributions are generated with increasingly different mean, in 1D and 2D.

Similar to the normal distribution, for the bimodal distributions shown in Figure 1.5 we find that the epsilon values do not increase linearly. There are two peaks

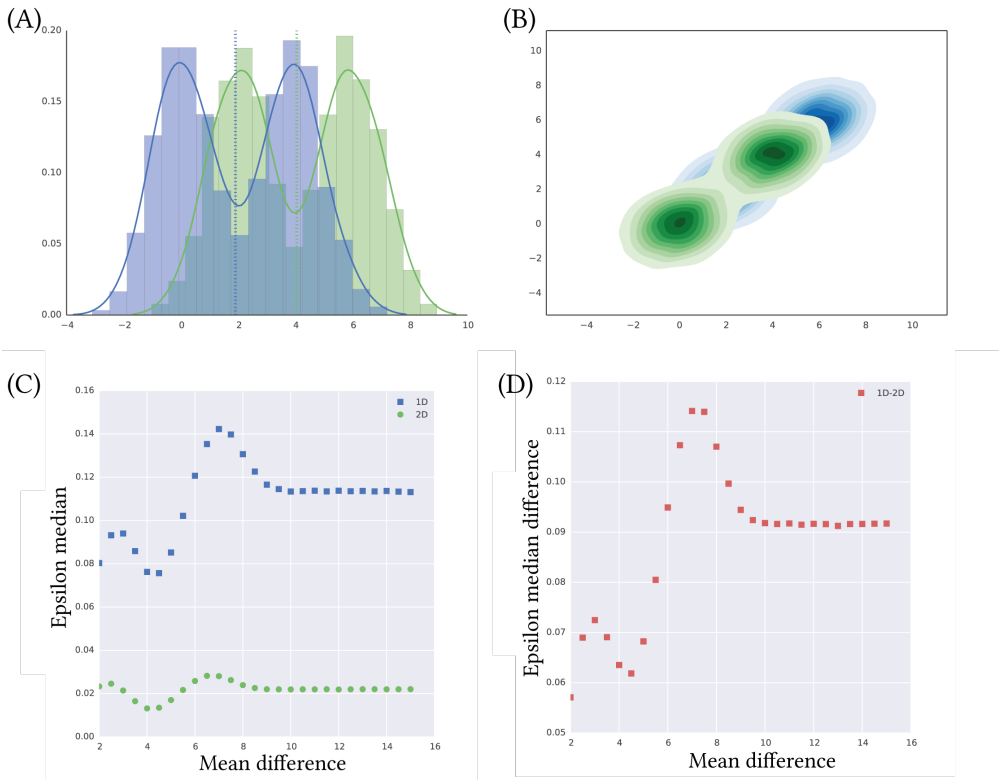

Figure 1.5 Comparing the 1D and 2D distances between bimodal distributions. (A) and (B) show samples of the bimodal distributions compared in 1D and 2D respectively with a mean difference of 4 between simulations and data. (C) The range by which epsilon median and variance varies as the difference between the mean of the distributions increases. (D) The difference between the epsilons calculated in 1D and 2D is not constant.

in the epsilon distribution, one at mean difference = 3 and one at mean difference=6. The epsilon values then decline until they reach a plateau. The epsilon values do not have a large range of values, for neither the 1D or 2D cases. We also find that the difference in the epsilon values between the 1D and 2D cases is not constant.

Finally, I study how these distance functions perform when comparing a bimodal with a normal distribution. A bimodal distribution is generated and a series of normal distributions with increasing mean, in 1D and 2D. From Figure 1.6 we find that epsilon is the lowest when the mean of the normal distribution corresponds to the μ of one of the two peaks in the bimodal distribution and the highest when there is no overlap between the distributions.

From Figures 1.4-1.6 I conclude that Algorithm 2 is not a good measure for distance to be used in ABC-Flow. If Algorithm 2 was used in order to minimize the

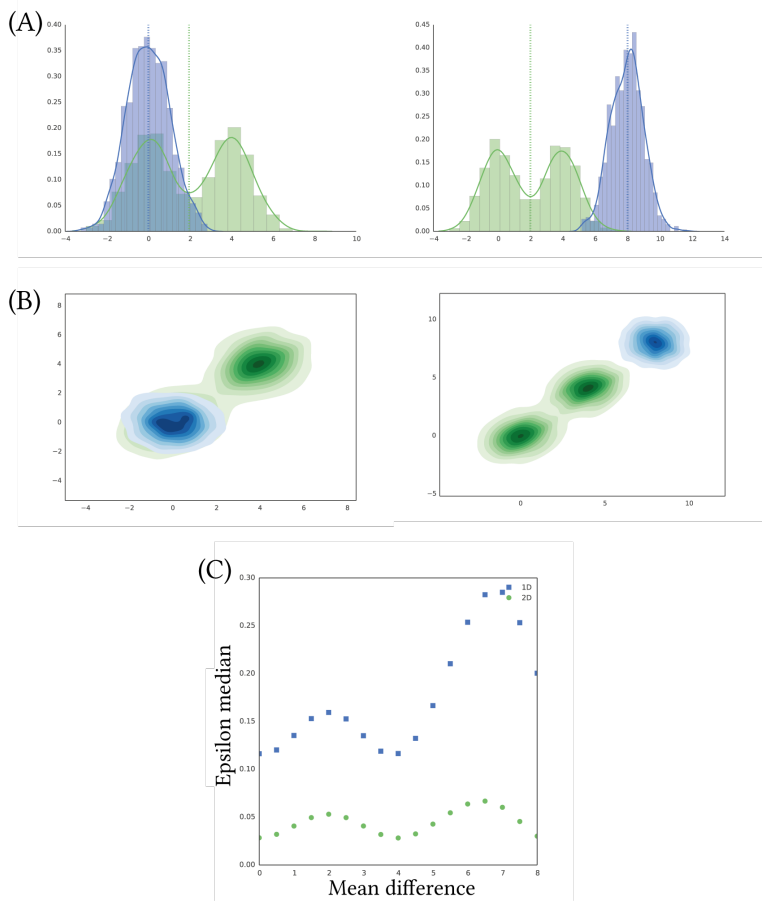

Figure 1.6 Comparing a multimodal to a normal distribution, in 1D and 2D. (A, B) The mean of the normal distribution is varied from equal to the mean of the first peak of the bimodal distribution to beyond the range of the bimodal distribution. (C) Epsilon median and variance are at the lowest when the mean of the normal distribution is equal to the mean of one of the peaks of the bimodal distribution.

distance between two distributions that start off with very different means, the distance between the two distributions will not be sufficiently minimized. This stems from the fact that ABC-FLow works by iteratively making the accepted epsilon smaller. As can be seen in Figure 1.4, if the two distributions have a large difference in the means, (>6) it would not be possible to overcome the peak that is created when the mean difference is at 3. Epsilon values increase before the decrease again, which will be a problem in ABC-Flow. Therefore a different distance calculation was developed.

1.4.2.2 Kolmogorov-Smirnov distance

In order to avoid the problems that arose from the distance calculation described in Section 1.4.2.1 I implemented a different distance calculation for ABC-Flow. I used a Python implementation of the Kolmogorov-Smirnov two sample test for the 1D case (Kolmogorov 1933). The Kolmogorov-Smirnov (KS) test is a non-parametric statistic test that determines whether two data sets were frawn from the same underlying distributions. The KS distance between two distributions is equal to the largest distance between the empirical distribution functions of the two samples, as shown in Equation 1.2.

$$D_{n,n'} = \sup_x |F_{1,n}(x) - F_{2,n'}(x)| \tag{1.2}$$

For the 2D case the distance was calculated by using the 2D Kolmogorov-Smirnov two sample test. The algorithm was developed by Fasano & Franceschini (1987) and the Python implementation developed by Major (2016).

This distance calculation was tested to determine whether it is an appropriate distance function to use in ABC-Flow. Two datasets were drawn from normal distributions with increasingly different means. The KS test was then used to calculate the distance between the data sets. This was carried out in 1D and 2D. The results are shown in Figure 1.7.

The epsilons of the 1D Kolmogorov-Smirnov distance calculation increase with increasing mean difference until it reaches a plateau when the two distributions are very different. This makes it an ideal distance calculation to be used in ABC-Flow. As the epsilon threshold is lowered at each iteration the difference between the two data sets decreases. Therefore the 1D KS statistic was used in ABC-Flow.

The multidimensional Kolmogorov-Smirnov test presents a challenge, as there is no unique way to order the data points to calculate the largest distance. There are $2^d - 1$ ways of ordering the data points and defining a cumulative distribution function, where d is the number of dimensions (Lopes, Reid, & Hobson 2007). This has affected the results of the computed distance seen in Figure 1.7. The variability in the calculation of the distance between data sets originating from distributions with known distance is large relative to the range of values the calculation can take. This was further confirmed when testing this distance on simulated data, where no parameter identifiability was observed (data not shown).

To alleviate the above shortcomings of the multi-dimensional generalisation of the Kolmogorov-Smirnov test, a different distance calculation was used for the 2D

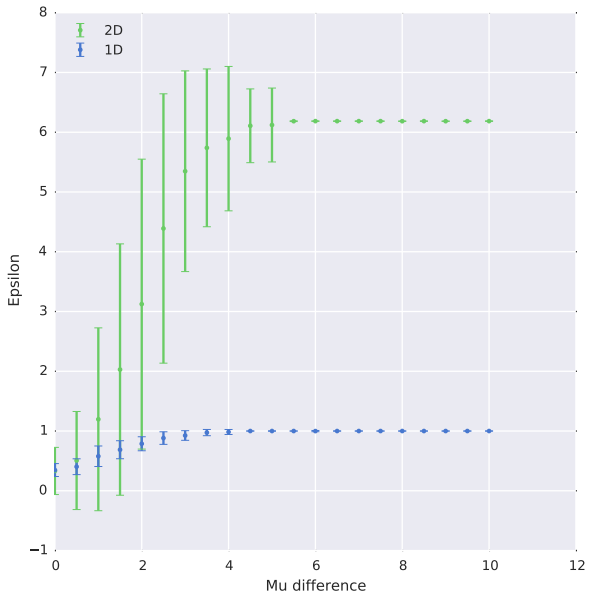

Figure 1.7 The Kolmogorov-Smirnov distance function was tested in 1D (blue) and 2D (green). Two data sets were generated with increasing mean difference, and the Kolmogorov-Smirnov two-sample test was applied to compute the distance between the two.

case. The Kolmogorov-Smirnov test for the 1D case was used in ABC-Flow as it performed well in the testing shown here.

1.4.2.3 Wald-Wolfowitz distance

For the 2D case the distance was calculated by using the multivariate Wald-Wolfowitz test (Friedman & Rafsky 1979). This is a generalisation of the Wald-Wolfowitz test proposed by (Wald & Wolfowitz 1940), a non-parametric test to determine whether two data sets were drawn from the same distribution. This test works by computing the minimum spanning tree of the pooled samples. Any edge whose nodes originated from different samples are removed, and the number of *runs* (R) is then defined by the number of disjointed subtrees (Friedman & Rafsky 1979). If the number of *runs* is small, then the null hypothesis that the two samples originated from the same distribution cannot be rejected. The quantity W for two samples, of length m and n, computed is given by:

$$W = \frac{R - 2\frac{mn}{N} - 1}{\sqrt{\frac{2mn(2mn-N)}{N^2(N-1)}}}, \tag{1.3}$$

where $N = m + n$ and R is the number of *runs*. A Python implementation of the multivariate Wald-Wolfowitz test by Monaco (2014) was used here. This is a variation to the Wald-Wolfowitz test that can be efficiently applied to larger data sets. The Python code used is given in Appendix (XXX).

Here I test this distance calculation in a similar way as Section 1.4.2.1. First, the two data sets are drawn from increasingly different distributions, and the distance between them calculated. As shown in Figure 1.8D, the 2D distance is 0 when the difference between the μ from which the two datasets are drawn from the same distribution. The distance calculation reaches a plateau at epsilon = 140 when the mean difference is 4 or larger. The 1D distance is also shown in Figure 1.8C in order to compare the two calculations, but the 1D distance was computed using the Kolmogorov-Smirnov distance described in Section 1.4.2.2.

To further study the distance calculation used in ABC-Flow, two normal distributions were simulated, with $\mu = 0$ and $\sigma = 1$ and distance between them calculated using the Kolmogorov-Smirnov test in the 1D case and the Wald-Wolfowitz test in the 2D case. Doing this multiple times, the expected variation in distance values for identical distributions can be calculated. This is the error that can be expected when measuring distance in ABC-Flow. As can be seen in Figure 1.9, the range of distance values obtained in the 1D case is small. For the 2D case, the distance values obtained vary more than in the 1D case, but it is still small relative to the range of values that the Wald-Wolfowitz test can take shown in Figure 1.8.

Using the Wald-Wolfowitz test the value of epsilon increases with increasing distance between the distributions with relatively small variability between repeats. Since the 2D Wald-Wolfowitz test performed well in the test carried out above, it was implemented in ABC-Flow as the distance function for the 2D calculations.

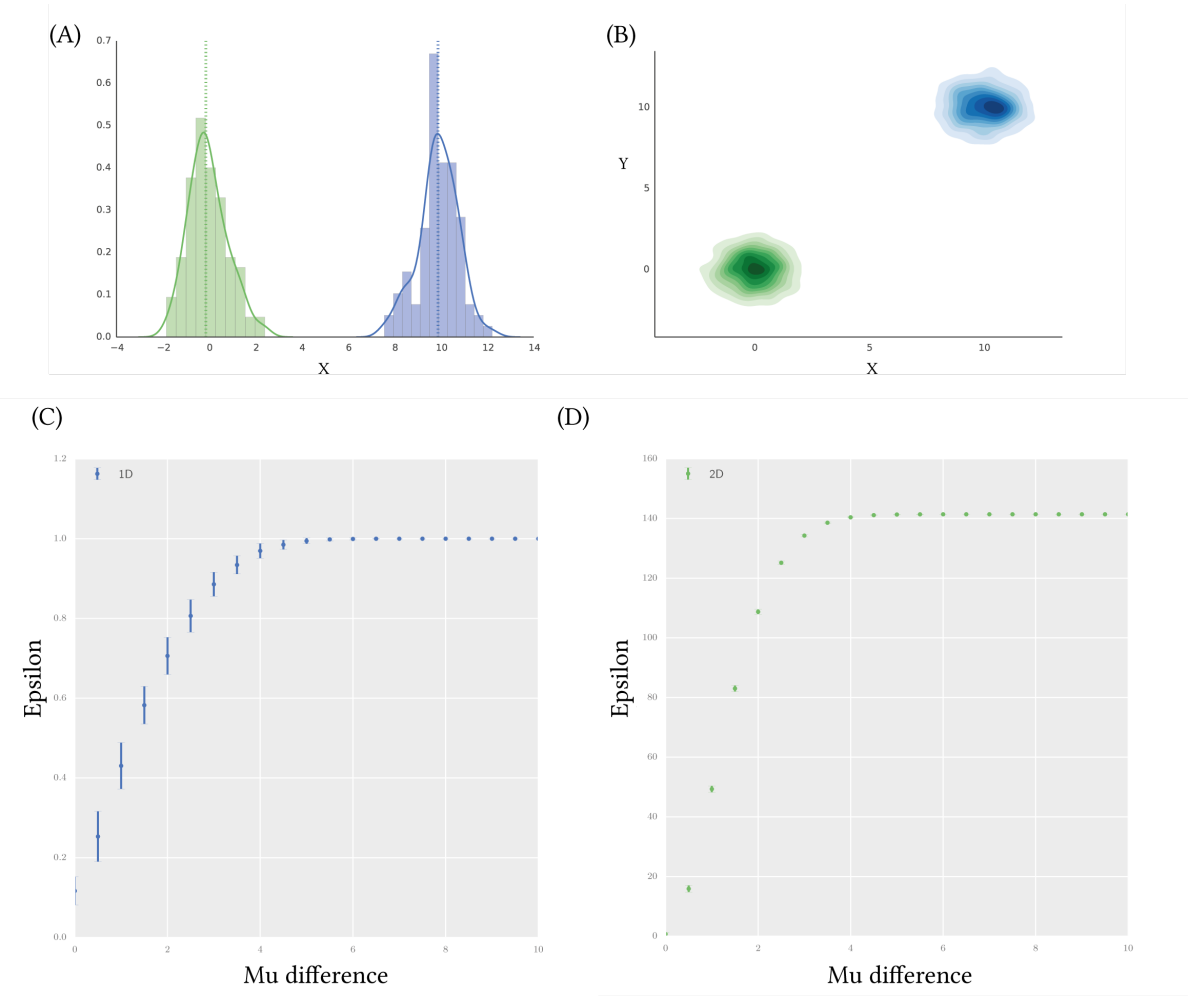

Figure 1.8 The distance calculation for data sets drawn from increasingly different distributions. Two examples are shown of distributions compared in (A) 1D and (B) 2D. (C) As the difference between the means of the two distributions increases, the distance calculation, epsilon, increases. In the 2D case (shown in green) epsilon plateaus at 2.3 and in the 1D case (shown in blue) epsilon plateaus at 1.

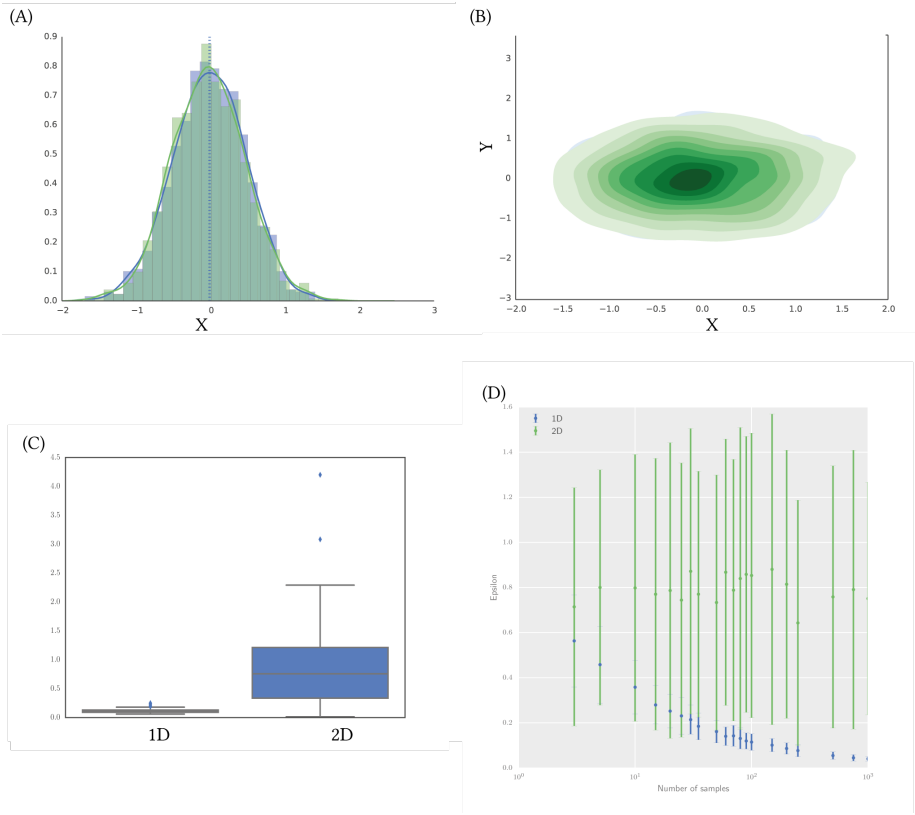

Figure 1.9 The distance between two data sets drawn form the same distribution are compared using the Kolmogorov-Smirnov two sample test. (A) in 1D and (B) in 2D. (C) The distance is calculated for 1000 data sets. A larger variation of values is found for the 2D distance calculation, but still small relative to the overall range of values. (D) As the number of samples in the datasets increase the distance calculation becomes more accurate in the 1D case. It has no effect on the 2D case.

1.5 ABC-Flow model fitting to simulated data

In this section I apply ABC-Flow to simulated data, where the parameter values used to produce the data are known. This analysis will serve as a verification test for ABC-Flow. The model used to produce the simulated data is an extension of the Gardner, Cantor, & Collins (2000) switch. The model consists of two mutually repressing transcription factors. The model used here has additional parameters allowing for gene expression to be leaky as well as include repression from an external stimulus.

In order to produce the simulated data set, an extension of the Gardner, Cantor, & Collins (2000) switch was simulated stochastically using the Gillespie algorithm (Gillespie 1977). The model used is defined by the following hazards:

$$h_1 = u \tag{1.4}$$

$$h_2 = \frac{p_1 p_3}{1 + p_3 + v^{p_2}} \tag{1.5}$$

$$h_3 = (1 + a) \times v \tag{1.6}$$

$$h_4 = \frac{p_4 p_6}{1 + p_6 + u^{p_5}}, \tag{1.7}$$

where u and v are the two proteins in the system, p_1 and p_4 represent the effective gene expression of u and v respectively, p_2 and p_5 represent the cooperativity of u and v respectively. p_3 and p_4 represent the leakiness of the promoters for each species. parameter α increases the degradation of one of the species, and simulates the addition of a repressor.

Using the time course data generated for one of the fluorescent proteins in the system, u, I use ABC-Flow to fit the model shown above, using priors centered around the parameter values used to produce the data, shown in Table 1.1. The resulting fit is shown in Figure 1.10A. In order to determine whether this is a good fit to the data, QQ plots are produced for each timepoint (Figure 1.10B). A QQ-plot is a plot where the quantiles of two distributions are plotted against eachother. If the distributions are similar, the points will lie on the 45° line x = y line (Wilk & Gnanadesikan 1968).

By examining the data and the fitted models shown in Figure 1.10, we see that at ε= 0.08, there is a good fit of the model to the data using ABC-Flow. The model parameters, as well as the intensity parameters, have been fitted to simulated flow cytometry data. The model has been successfully fitted to the simulated data. This is highlighted in the QQ plots in Figure 1.10B, where the results lie in the x=y line.

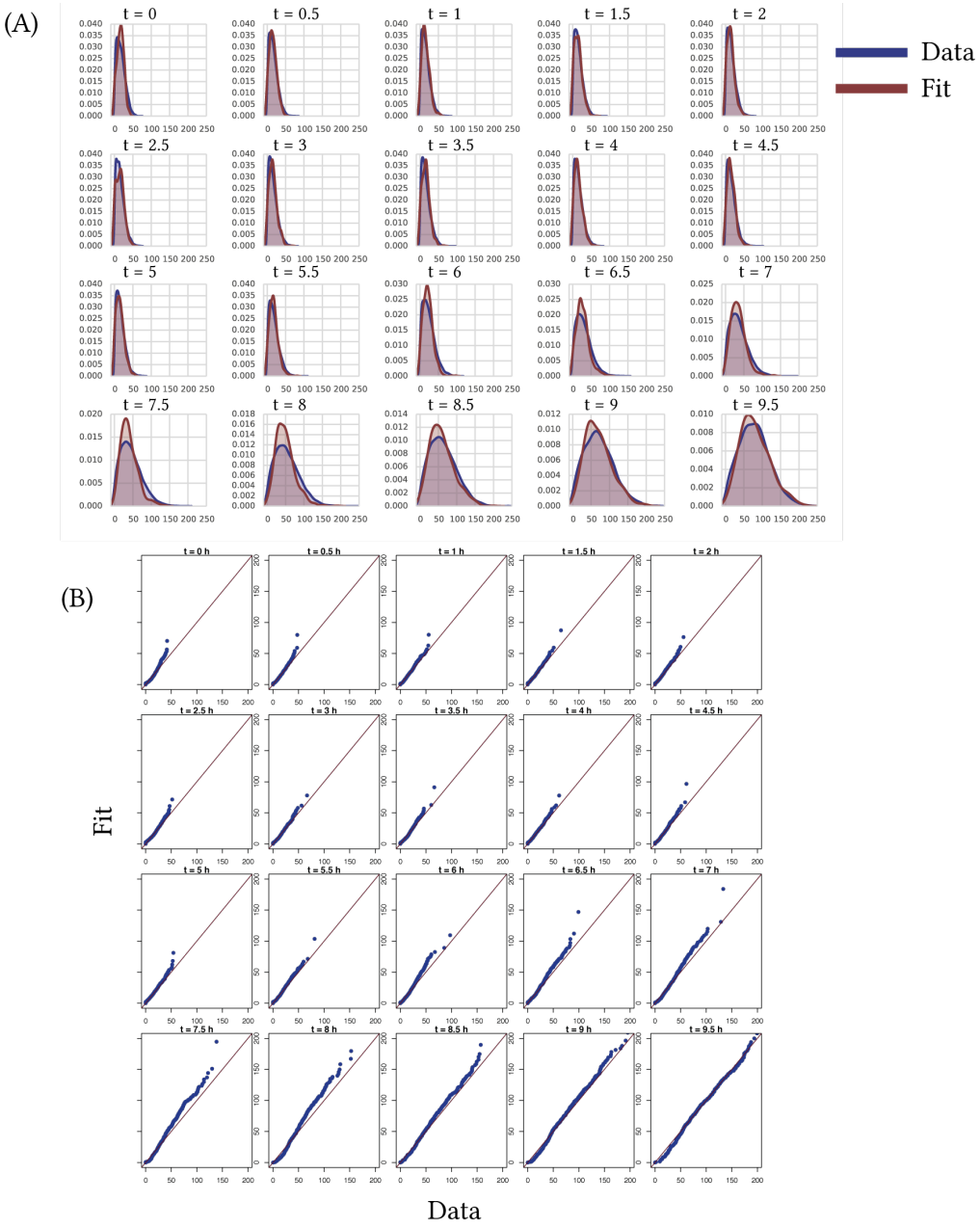

Figure 1.10 (A) 1D ABC-Flow fit (shown in blue) to data (shown in red) produced by simulating the same model. (B) QQ-plot of each time point fit. The quantile of the two distributions are plotted against eachother. If the ditributions are similar, the points would lie on the 45° line x = y, shown in red.

I further test ABC-Flow by using 2D data to fit two species of the model simultaneously. The same data was used as was used in the 1D case, but this time both species u and v were taken into account. This represents both sides of the switch model used.

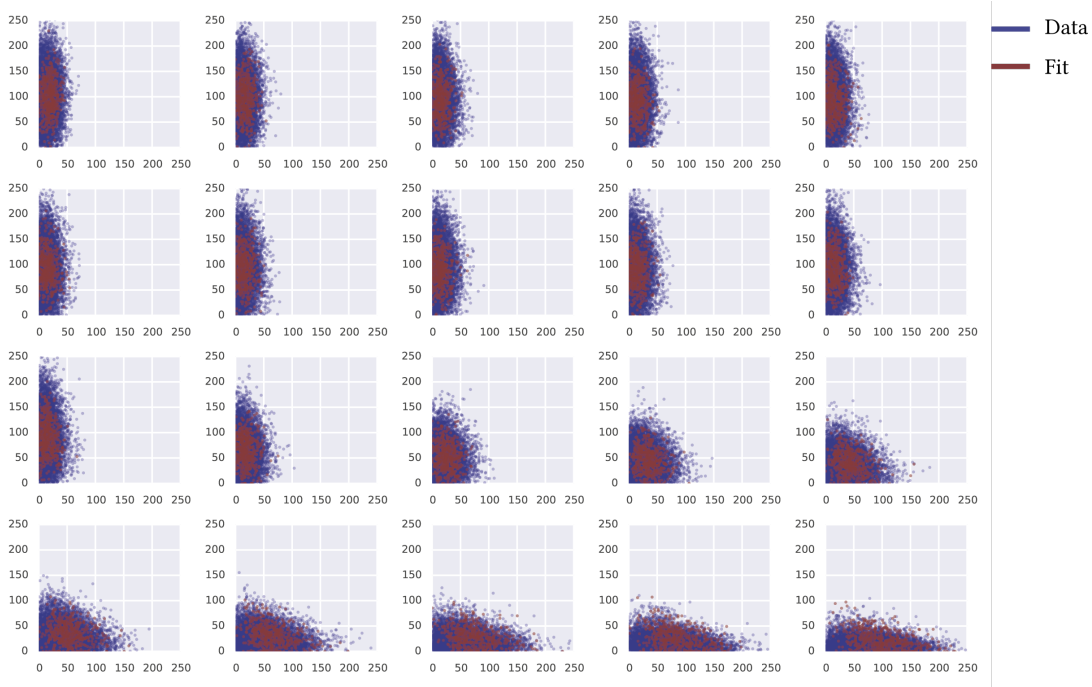

Figure 1.11 2D ABC-Flow fit (shown in blue) to data (shown in red) produced by simulating the same model.

The posterior distributions obtained from each fit are shown in Figure 1.12. We find similar posterior ranges for both the 1D and 2D fits. Both fits identified the parameters necessary to produce the simulated data. From the posteriors we find that the most constrained parameters to produce the switch behaviour in this model are parameters $p2$ and $p5$, the parameters representing the cooperativity of the repressors. They both have to be equal to 2 to produce the observed behaviour in this model. We also find that α, the parameter representing the increased degradation of the repressing species due to the addition of an inducer, is tightly constrained. α is required to be small. Further, we find that μ and σ, the parameters representing the mean and standard deviation of the fluorescence intensity emitted by each fluorescent molecule to be tightly constrained.

These results demonstrate that ABC-Flow can successfully fit a computational model to flow cytometry data. It can identify the parameter values necessary to

(A)

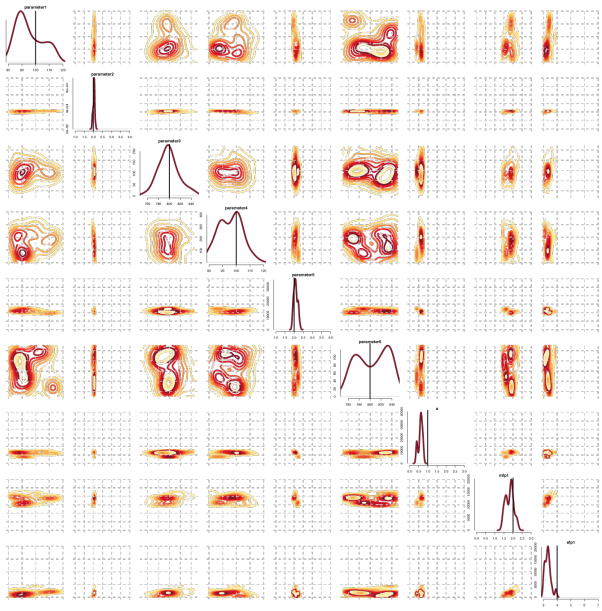

(B)

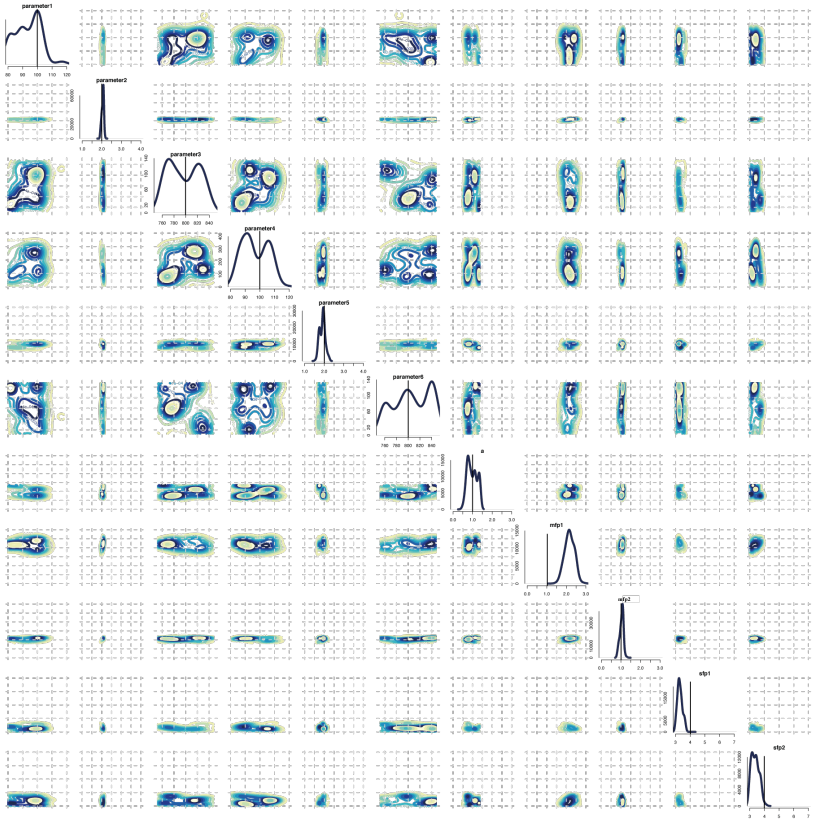

Figure 1.12 The posterior distributions of the 1D (red) 2D (blue) fits to simulated data. The parameters used to produce the simulated data set were identified in both cases.

Table 1.1 The priors used for the 1D and 2D ABC-FLow model fitting to simulated data

Parameters		
	1D	2D
p1	30 - 150	30 - 150
p2	1 - 5	1 - 5
p3	700 - 850	700 - 850
p4	30 - 150	30 - 150
p5	0 - 5	0 - 5
p6	700 - 850	700 - 850
p7	0 - 5	0 - 5
Species		
u	9 - 11	9 - 11
v	90 - 110	90 - 110
Intensity parameters		
mean fp1	0 - 5	0 - 5
mean fp2		0 - 5
sigma fp1	0 - 7	0 - 7
sigma fp2		0 - 7

produce the observed behaviour. ABC-Flow can now be confidently applied to real flow cytometry data of the genetic toggle switch. This will allow me to fit a computational model to experimental data of the genetic toggle switch and uncover the parameters that are necessary to produce this behaviour. In the following Section I will outline the methods used to obtain the experimental data necessary and the results obtained.

1.6 Toggle switch data collection

In this section I collect experimental data on the genetic toggle switch. Using flow cytometry and the necessary inducers to flip the switch I study the switch flipping over time as well as over different inducer concentrations.

1.6.1 Circuit overview

The toggle switch plasmid I used here was provided by Litcofsky et al. (2012). All the switch components were contained in one plasmid, pKDL071. An overview of the plasmid is shown in Figure 1.13A and the sequence given in Appendix (XXX). The circuit consists of two promoters, Ptrc2 and PLtetO-1 (Lutz & Bujard 1997). Ptrc2 is a constitutive promoter, repressible by LacI. PLtetO-1 is also a constitutive promoter, repressible by TetR, as shown in Figure 1.13B. mCherry (Shaner et al. 2004) and GFP (Shimomura, Johnson, & Saiga 1962) are fluorescent proteins, that were added under the control of the same promoters as the repressors, and thus reflect the levels of TetR and LacI in the system. The plasmid contains kanamycin antibiotic resistance and is high copy (ColE1 origin of replication).

This system is capable of two states, GFP high and mCherry high. When IPTG is added to the system, it represses the repression of TetR and mCherry and thus the cells end up in the mCherry high state. When ATc is added to the system, it represses the repression of LacI and GFP and thus the cells end up in the GFP high state. If no inducer is added to the system it will randomly go to the GFP high or mCherry high states.

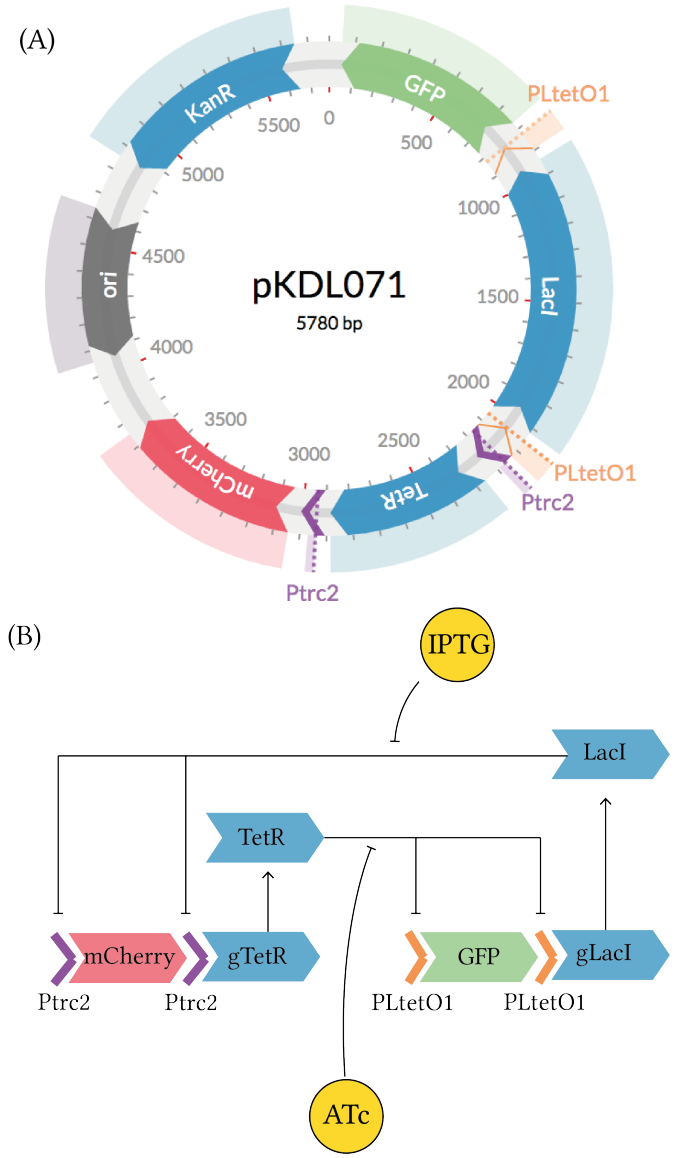

Figure 1.13 : The genetic toggle switch circuit used in this chapter. (A) The plasmid map of pKDL071, the plasmid containing the genetic toggle switch used in Litcofsky et al. (2012) (B) The interactions between each element of the circuit.

1.6.2 Methods

The toggle switch plasmid was provided by the James J Collins lab in the form of a stab culture in *E. coli* K-12 MG1655.

1.6.2.1 *Escherichia coli* culturing conditions

Lysogeny broth (LB) was made by diluting LB in deionized water to a concentration of $25\,\mathrm{g\,L^{-1}}$ and subsequently autoclaved. LB agar plates were made by adding bacteriological agar to the above solution to a concentration of $45\,\mathrm{mg\,mL^{-1}}$ before autoclaving. The solution was then cooled down to 55 °C using a water bath. If antibiotic was required it was added to the correct concentration to the cooled solution. The solution was then aliquoted to plates and left to solidify in room temperature. The plates were stored in the fridge for up to 1 month.

Overnight cultures were made by picking a single colony from a static culture in an agar plate. Each colony was placed in 15 mL Falcon tubes (Fisher Scientific, MA, U.S.A) with 5 mL LB with kanamycin antibiotic at a concentration of $50\,\mathrm{\mu g\,mL^{-1}}$. The tubes were then screwed loosely and taped securely in order to allow for aeration. The falcon tubes were put in an incubator at 37 °C with orbital shaking at 200 rpm for 12-16 hours.

1.6.2.2 Glycerol stock preparation

To preserve the transformed cultures long-term glycerol stocks were made. 5 mL LB and Kanamycin overnight cultures were made as described in Section 1.6.2.1. The cultures were kept on ice and 70 % glycerol was added to the cultures in a ratio of glycerol to culture of 1:7. These were aliquoted into cryovials and transferred to a −80 °C freezer for long-term storage.

1.6.2.3 Revival

For subsequent revival of the frozen cultures, a 1.5 mL eppendorf tube was removed from the −80 °C freezer and put on ice. Small amount was streaked onto an agar plate containing LB and kanamycin. The plates were stored in an incubator at 37 °C overnight. Then the plates were sealed using parafilm and stored at 4 °C for up to two weeks.

1.6.2.4 Plasmid construction

Plasmids were constructed via PCR cloning. PCR primers were chosen to add restriction enzyme sites on the 5' and 3' were needed. Following PCR amplification, the amplified DNA was purified using the Qiagen PCR cleanup kit (Qiagen, Crawley, U.K). Double digests were carried out and the desired fragment isolated via gel extraction. The relevant fragments were subsequently ligated. Following construction, each plasmid was isolated using the QIAprep Spin Miniprep Kit (Qiagen, Crawley, U.K). Plasmid concentration was determined using the Thermo Scientific NanoDrop 1000 Spectrophotometer (Fisher Scientific, MA, U.S.A).

1.6.2.5 Polymerase Chain Reaction

In order to amplify DNA and add the restriction enzyme sites required, a Polymerase Chain Reaction (PCR) reaction was carried out with mutagenic primers. A list of primers can be found in Appendix (XXX). Q5® DNA Polymerase (NEB, MA, U.S.A) was used with its associated buffer, dNTPs and Q5® enhancer, as specified in Table 1.2. PCR reactions were run in a T100™ thermal cycler (Bio-Rad Laboratories, Inc., UK) as per the Q5® recommendations, and as outlined in Tables 1.2 and 1.3.

Table 1.2 PCR recipe

Reagent	Final concentration	50 µL reaction
Q5® buffer 5X	1X	10 µL
dNTPs	200 mM each	1 µL
Forward primer	0.5 µM	2.5 µL
Reverse primer	0.5 µM	2.5 µL
Template DNA	2 µg/50 µL	-
Q5® DNA polymerase	0.02 U μL^{-1}	0.5 µL
Q5® enhancer	1X	10 mL
H_2O	-	to 50 µL

Table 1.3 Thermocycling conditions

Step	Cycles	Temperature	Time
Initiation	1	98 °C	30 s
Denaturation		98 °C	10 s
Annealing	30	72 °C	20 s
Extension		72 °C	2 min
Final extension	1	72 °C	2 min
Hold	1	4 °C	∞

1.6.2.6 Digestion

All enzymes, buffers and Bovine Serum Albumin (BSA) were supplied by NEB. Digestion controls were carried out by adding H_2O instead of DNA in the digestion reaction. Additionally, during agarose gel electrophoresis uncut plasmid was run alongside the digested plasmid in order to detect the difference.

2 µg digests were set up by mixing the plasmid with 0.5 µL of each restriction enzyme, 3 µL 10x buffer and 3 µL 10x BSA. H_2O was added to make the reaction to 20 µL. The recipe used is shown in Table 1.4. The reactions were placed in an incubator at 37 °C for 4 hours. Finally, the solutions were analysed using agarose gel electrophoresis (Section 1.6.2.7).

Table 1.4 Digestion recipe

Reagent	Volume
PstI	0.5 µL
HindIII	0.5 µL
NEB Buffer 2.1	2 µL
BSA	0.2 µL
DNA	1 µg
H_2O	to 20 µL

1.6.2.7 Agarose gel electrophoresis

To make a 0.8% agarose gel, 0.4 g agarose were diluted in 50 mL 1X TAE buffer. It was further dissolved by microwaving for 1-3 minutes. The solution was left to cool for 5 minutes and then 1.5 µL gel red were added. Gel trays were prepared by putting the well comb in place and taping the ends shut. The solution wast then

poured into the prepared gel trays and left to solidify for 20-30 minutes at room temperature.

Agarose gel electrophoresis was carried out by placing the poured gels into the gel tanks. The tank was then flooded with 1X TAE buffer. The DNA was prepared to be analysed by adding 4 µL loading dye to 20 µL sample. A negative control was used with H_2O instead of sample. The DNA ladder of choice was prepared by adding 1 µL H_2O and 1 µL dye to 2 µL ladder. Each sample was added to a well by pipetting. The agarose gel was ran at 90 V until the dye was 80% of the way down the gel, approximately 1 hour.

To purify the fragments from the agarose gel, the gel was placed in a UV box. Using a sterile razor blade, the desired fragment was cut out and placed in a clean eppendorf tube. The DNA was isolated from the gel using the QIAquick Gel Extraction Kit.

1.6.2.8 Ligation

A ratio of 3:1 of insert to recipient plasmid was used, 1 µL T4® DNA ligase (NEB, MA, U.S.A) and 2 µL ligase buffer. H_2O was added to make the reaction up to 20 µL. The controls used for each ligation reaction, are shown in Table 1.5. Control 1 is used to detect competent cell viability, control 2 background due to uncut vector, control 3 contamination and control 4 vector re-circularization.

The ligation reactions were placed at 4 °C for 12 hours. The reactions were then placed at 65 °C for 10 minutes to heat inactivate the T4 DNA ligase enzyme. A transformation was then carried out as per Section 1.6.2.9.

Table 1.5 Ligation controls

	Control 1	Control 2	Control 3	Control 4
Vector	Uncut	✓	✓	✗
Insert	✗	✗	✗	✓
Buffer	✓	✓	✓	✓
H_2O	✓	✓	✓	✓
Ligase	✗	✗	✓	✓

1.6.2.9 Transformation

Thermocompetent *E.coli* Dh5α was transformed with the constructed plasmids. Each ligation reaction was added to 50 µL of thawed competent cells. The cells were sub-

sequently kept on ice for 30 minutes, then placed at a 42 °C water bath for 45 s. The cells were then placed back on ice for 15 minutes. Then 500 µL of Super Optimal broth with Catabolite repression (SOC) were added to each ligation and placed in a 37 °C shaking incubator for 3 hours. 500 µL and 50 µL were subsequently pipetted of each ligation onto petri dishes with LB agar and the appropriate antibiotic. The plates were incubated at 37 °C for 12-16 hours. Two controls were used for the transfection protocol, a positive control with no antibiotic in the LB agar and non-transfected cells and a negative control of non-transformed cells and LB agar with antibiotic. These ensure that the cells are viable and not contaminated respectively.

Finally, the number of colonies were counted on each plate. Individual colonies were then selected from each transfection and grew each separately in 5 mL LB medium for 12-16 hours at 37 °C, 200 rpm. Glycerol stocks were then prepared from each culture, as per Section 1.6.2.2.

1.6.2.10 Colony PCR

In order to determine if the fragment was successfully inserted into the vector DNA plasmid, diagnostic colony PCR was then carried out. Primers were designed that amplified the multiple cloning site of the vector DNA plasmid. These can be found in Appendix (XXX). A PCR master mix was made for the number of colonies to be amplified, 32, with an added 10% to account for pipetting error. GoTaq® Flexi DNA polymerase (Promega Corp., WI, U.S.A.) was used with its associated buffer, dNTPs and $MgCl_2$and H_2O. The recipe for the master mix is shown in Table 1.6.

Table 1.6 Colony PCR master mix recipe

Reagent	Final concentration	Master mix
GoTaq® green Flexi buffer	1X	141 µL
dNTPs	200 mM each	14.1 µL
Forward primer	0.5 µM	1.4 µL
Reverse primer	0.5 µM	1.4 µL
GoTaq® Flexi polymerase	0.02 U μL^{-1}	3.5 µL
$MgCl_2$	1X	42.2 µL
H_2O	-	465 µL

19 µL were then added from the master mix to each PCR tube. Each of the colonies was then lifted from the transformation from the agar plate using a 20 µL pipette tip and added it to a PCR mix by mixing. The pipette tip was subsequently used to

make a scratch into a clean agar plate, and labelled it. A PCR was then carried out according to GoTaq® Flexi polymerase recommendations, and as shown in Table 1.7.

Table 1.7 Thermocycling conditions for colony PCR

Step	Cycles	Temperature	Time
Cell lysis	1	95 °C	10 minutes
Denaturation		95 °C	30 s
Annealing	35	50 °C	1 minute
Extension		72 °C	1 min
Final extension	1	72 °C	5 min
Hold	1	4 °C	∞

Finally a diagnostic agarose gel electrophoresis was carried out as outlined in Section 1.6.2.7.

1.6.2.11 Sequencing

In order to confirm plasmid identity, all plasmids were sequenced using Source Bioscience, Cambridge UK. 10 µL of each plasmid DNA were submitted at a minimum of 100 ng μL^{-1} as per the requirements. Primer sequences were also submitted and manufactured by Source Bioscience. Primers can be found in Appendix (XXX).

1.6.2.12 Inducers

Anhydrotetracycline (ATc) solution was made by diluting ATc from Cayman Chemical Company in 100 % ethanol to a concentration of 1 mg mL^{-1}. Isopropyl-beta-D-thiogalactopyranoside (IPTG) solution was made by dissolving IPTG in deionized water to a concentration of 1 M. The solution was sterilised by passing the solution through a 0.22 µm syringe filter. Both inducers were stored in 1 mL aliquots at −20 °C.

1.6.2.13 Growth rate measurement

Plate reader analysis was carried out in order to measure the growth of *E.coli* over time. Overnight cultures were made using the method shown in Section 1.6.2.1. Overnight cultures were then diluted by a 1:1000 ratio into a 5 mL LB + kanamycin solution. The diluted cultures were grown at 37 °C with shaking at 200rpm for 1 hour. These cultures were then further diluted by a 1:100 ratio. 200 µl aliquots of the dilutions were then transferred to a clear bottom, black-walled 96-well plate.

Wells with only LB and kanamycin were also added in order to be used as blanks. The plate was then sealed using a gas permeable membrane and placed it in BMG FLUOstat OPTIMA plate reader to measure absorbance. The plate reader was set to a constant 37 °C, with 30 seconds orbital shaking at 150 rpm and 4 mm shaking width every ten minutes. Absorbance was measured at 540 nm. Data was exported as a CSV file and analysed using Python.

1.6.2.14 Flow cytometry

Flow cytometry experiments were carried out in order to get fluorescent levels in single cells. Flow cytometry allows us to gather this information for thousands of single cells. Flow cytometry data was exported as FCS files and analysed using the R bioconductor packages flowCore (Ellis et al. 2016b), flowViz (Ellis et al. 2016a) and Ggplot2 (Wickham 2009). Prior to analysis the raw data was processed to remove any debris or instrument noise detected. The data was also processed to removed any doublets, which occurs when more than one bacterial cell passes through the detector at a time. This will skew the data by including datapoint with double the fluorescent intensity that the rest of the population. The pre-processing was done by using the side scattering data. The height and the area of the sample forward scattering distribution is recorded during an experiment. The cells that lie in the diagonal where the area equals the height are single bacterial cells. If the area of the signal exceeds the height it is indicative of a doublet, or cluster of cells, and is removed from the data. This preprocessing was carried out using autoGate, developed by Fedorec (2016).

1.6.2.15 Concentration assays

Concentration assays were carried out in order to determine the concentration of each inducer (ATc and IPTG) at which the switch flips. Separate overnight cultures were prepared as per Section 1.6.2.1 with added IPTG at a concentration of 1 mM or added ATc at a concentration of 100 ng mL^{-1} (Litcofsky et al. 2012). The cultures were then diluted by 1:1000 into fresh LB medium with varying concentrations of the opposite inducer than what the cells were grown in overnight. The concentrations used are shown in Table 1.8. For each concentration. three replicates cultures were made.

The cultures were placed in an incubator at 37 °C, 200rpm for 5 hours. The cultures were then placed in a centrifuge and spun at 13,000rpm for 5 minutes. The supernatant was discarded and replaced it with 1 mL PBS solution. The BD

Table 1.8 Concentrations used for flow cytometry assay

ATc (ng/ml)	IPTG (M)
0.05	1e-7
0.06	6e-7
0.07	1e-6
0.08	6e-6
0.09	1e-5
0.1	1e-3
1.0	0.1

LSRFortessa^{TM} cell analyzer (Becton, Dickinson and Company) was used at the St. Mary's Flow Cytometry Core Facility at Imperial College London for flow cytometry analysis. GFP was excited using the 488 nm laser and detected using the 533/30 filter. mCherry was excited using the 561 nm laser and detected using the 620/10 filter. Data was obtained at n=10000 events per experiment.

1.6.2.16 Time course assays

Time course assays were carried out to measure the time it takes for the switch to flip to each state. Separate overnight cultures of pKDL071 were prepared as per Section 1.6.2.1 with added IPTG at a concentration of 1 mM or added ATc at a concentration of 100 ng mL^{-1} (Litcofsky et al. 2012). Overnight cultures of pSEVA281G and pSEVA281C were also made. The cultures were then diluted by a ratio of 1:1000 into fresh LB medium. Separate cultures for each time point were made, in triplicate. For cultures grown overnight in IPTG, ATc was added at a concentration of 100 ng mL^{-1} and for cultures grown overnight in ATc, IPTG was added at a concentration of 1 mM. All cultures were placed at 37 °C, 200rpm incubator. At 30 minutes, 1 hour and then every hour up to 6 hours flow cytometry was carried out for the corresponding cultures. Triplicates for each induction were removed from the incubator and placed in a centrifuge at 13, 000rpm for 10 minutes. The supernatant was discarded and replaced with 1 mL PBS solution. These cultures were then analysed in an Attune^{TM} NxT Flow Cytometer (Thermo Fisher Scientific) at University College London. GFP was excited using the 488 nm laser and detected using the 533/30 filter. mCherry was excited using the 561 nm laser and detected using the 620/10 filter. Data was obtained at n=10000 events per experiment. pSEVA281G and pSEVA281C cultures were used to set the laser voltages and pKDL071 cultures to detect the bacteria population.

1.6.3 Results

1.6.3.1 pKDL071 plasmid alteration

The pKDL071 plasmid contains all the elements of the switch. The two states of the switch are LacI high and TetR high. These are detected by using the fluorescent proteins that are controlled by the same promoters, and thus mirror the levels of LacI and TetR. The concentration of LacI can be estimated by GFP intensity and TetR concentration by mCherry intensity. In order to detect GFP and mCherry levels within each cell simultaneously, flow cytometry can be used. The lasers needed to excite GFP and mCherry are 488 nm blue and 561 nm yellow respectively. Since the blue laser was not available for use in the BD Acuri^{TM} C6 or the BD LSRII^{TM} (Becton, Dickinson and Company) flow cytometers available, an alternative construct had to be made in order to be able to detect the levels of both sides of the switch.

In order to alter the switch construct to be able to detect both sides, the mCherry gene was swapped for the YFP gene. The yellow fluorescent protein is excited by the blue laser and could thus be detected using the equipment available. The YFP gene was available from BioBrick registry of standard biological parts as BBa_K592101. PCR cloning was used to introduce the flanking sequences of EcoRV and KasI restriction enzymes in the 5' and 3' ends respectively. The primers used are given in Appendix (XXX). A double digest was performed on plasmids pKDL071 and BBa_K592101, as well as positive and negative controls. Following gel extraction and ligation, the pKDL071-YFP plasmid was complete. The plasmid map is shown in Figure 1.14.

GFP and YFP have overlapping emission spectra, which have to be compensated during flow cytometry data acquisition (Shapiro 1941). This is because the signal from GFP can be detected at the YFP detector and vice versa. Due to the high level of compensation needed to be carried out and the relatively dim signal given by the bacteria used here, the different stages of the switch, ON and OFF, could not be resolved (data not shown). In order to be able to acquire toggle switch flow cytometry data, an alternative facility was found that was able to detect GFP and mCherry fluorescence.

1.6.3.2 Control plasmids construction

I constructed two plasmids in order to use them for the flow cytometry mCherry/GFP experiments. The first plasmid, pSEVA281G contains the promoter PLtetO-1 and GFP and the other, pSEVA281C, contains the promoter Ptrc2 and mCherry from

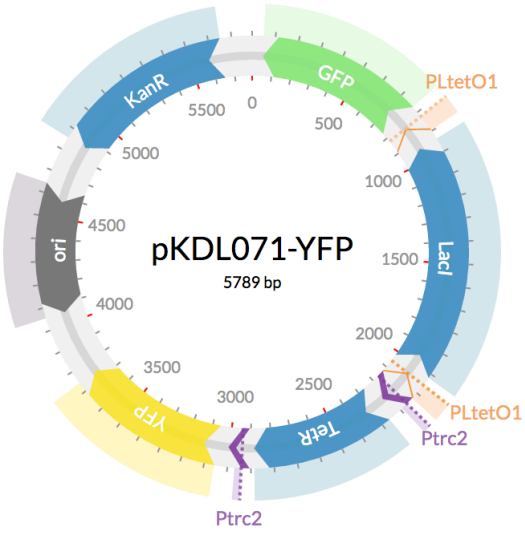

Figure 1.14 : pKDL071-YFP plasmid map.

PKDL071, shown in Figure 1.15. These two plasmids were used to determine the appropriate voltages for the lasers that excite GFP and mCherry.

pSEVA281G was constructed by digesting pKDL071 and pSEVA281 using the protocol outlined in Section 1.6.2.6. pSEVA281 is a plasmid backbone containing kanamycin resistance, a high copy origin of replication and a multiple cloning site. The digested fragments were isolated using gel purification (Section 1.6.2.7) and then ligated the isolated fragments (Section 1.6.2.8). *Escherichia coli* Dh5α was then transformed with each plasmid (Section 1.6.2.9).

pSEVA281C was constructed via PCR cloning. PCR was carried out using the pKDL071 plasmid as a template DNA using the protocol outlined in Section 1.6.2.5. Primers were chosen so that Ptrc2 and mCherry were copied and a HindIII restriction enzyme recognition sequence added to the fragment. The rest of the cloning procedure followed as per plasmid pSEVA281G.

1.6.3.3 Growth rate investigation

I carried out a growth rate analysis to determine whether the ATc or IPTG added to pKDL071 or pSEVA281G *E. coli* cultures affected the growth of the bacteria. Cultures were grown without any inducer overnight as described in Section 1.6.2.13. Assays for the cultures were ran with and without added inducers. As can be seen in Figure 1.16, there is no difference between the conditions. The addition of either ATc or IPTG does not affect the growth rate of *E. coli* K-12 MG1655. Additionally,

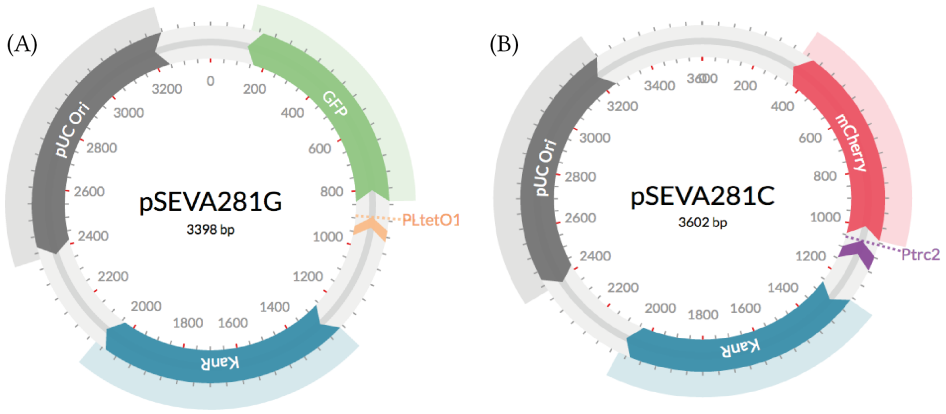

Figure 1.15 : The plasmids used to calibrate GFP and mCherry fluorescence. (A) pSEVA281G plasmid map (B) pSEVA281C plasmid map.

ATc does not affect the growth rate of *E. coli* Dh5α. Since the addition of ATc flips the switch to the GFP high state, and IPTG to the mCherry high state, we can also conclude that the growth rate of the chassis is not affected by which side of the switch is in the high state. The growth rate of *E. coli* Dh5α was consistently lower than that of *E. coli* K-12 MG1655.

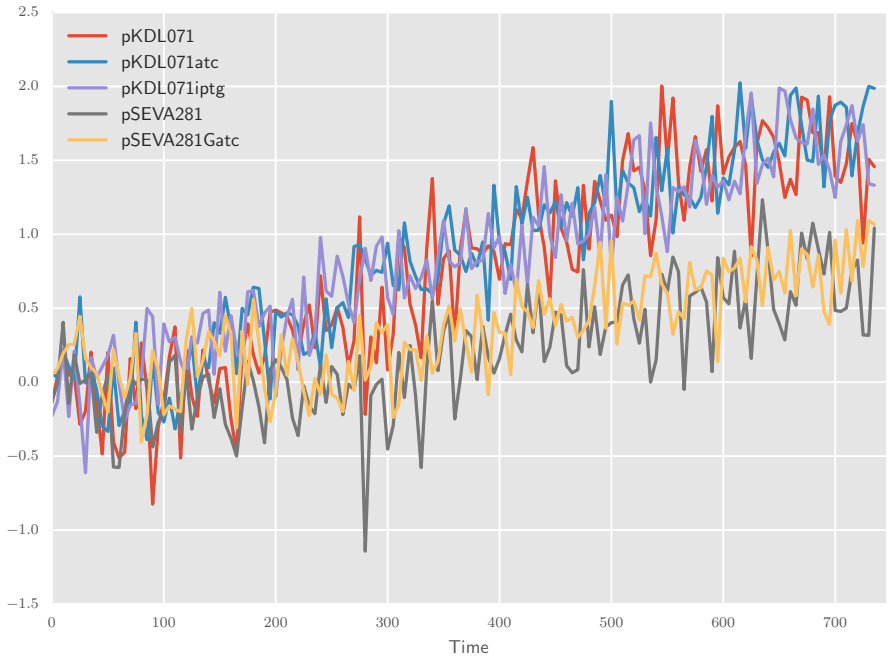

Figure 1.16 : Growth rate analysis of *E. coli* K-12 MG1655 pKDL071 and *E. coli* Dh5α pSEVA281G cultures with and without inducers. The inducers do not affect the growth of the bacteria.

1.6.3.4 Toggle switch concentration assays

Here I aim to identify the inducer concentration at which the pKDL071 toggle switch changes state. In order to do that I carry out a concentration assay using flow cytometry, as described in Section 1.6.2.15. As can be seen in Figure 1.17A, during ATc induction the switch flips to a GFP high state when ATc concentration is at 0.09 ng mL^{-1} or higher. We observe a bimodal distribution at concentrations 0.07 ng mL^{-1} and 0.08 ng mL^{-1}, which indicates that the switching has begun at these concentrations. Thats why part of the population has switched to the GFP high state but complete switching is not observed until the concentration of ATc is at 0.09 ng mL^{-1}. In the case of IPTG induction (Figure 1.17B) we find that the switch flips to the mCherry high state when the concentration of IPTG is higher or equal to 0.001M. A decrease in GFP fluorescence is also observed. We do not observe a bimodal distribution in this case.

The Hill function, given below, was used to obtain the characterization curves of the two inductions, ATc and IPTG.

$$F = Pmin + (Pmax - Pmin)\frac{\left(\frac{[I]}{Kd}\right)^n}{1+\left(\frac{[I]}{Kd}\right)^n}, \tag{1.8}$$

where F is the median fluorescent unit and [I] is the concentration of inducer. Pmin and Pmax are the minimum and maximum fluorescence respectively, and Kd and n are the dissociation constant, and Hill coefficient. I fit the Hill function by using the nonlinear least squares estimation in the R statistical environment (Team 2008). Initial values used for the Hill function parameters P_{min}, P_{max}, K_d, and n are given in Table 1.9.

Table 1.9 Initial values used for Hill function parameters

	pmin	pmax	kd	n
ATc induction	18	1800	0.12	2
IPTG induction	0	800	0.00001	1.6

For the case of the ATc induction we observe a sharp switch between the GFP low to the GFP high state, as can be seen in the characterisation curve in Figure 1.18B. This sharp switch made the fitting of the Hill function challenging. The parameters producing the best fit of the Hill function found are $P_{min} = 18.3$, $P_{max} = 1541.3$, $K_d = 0.097$, and $n = 56.7$. The cooperativity parameter n is very high in this

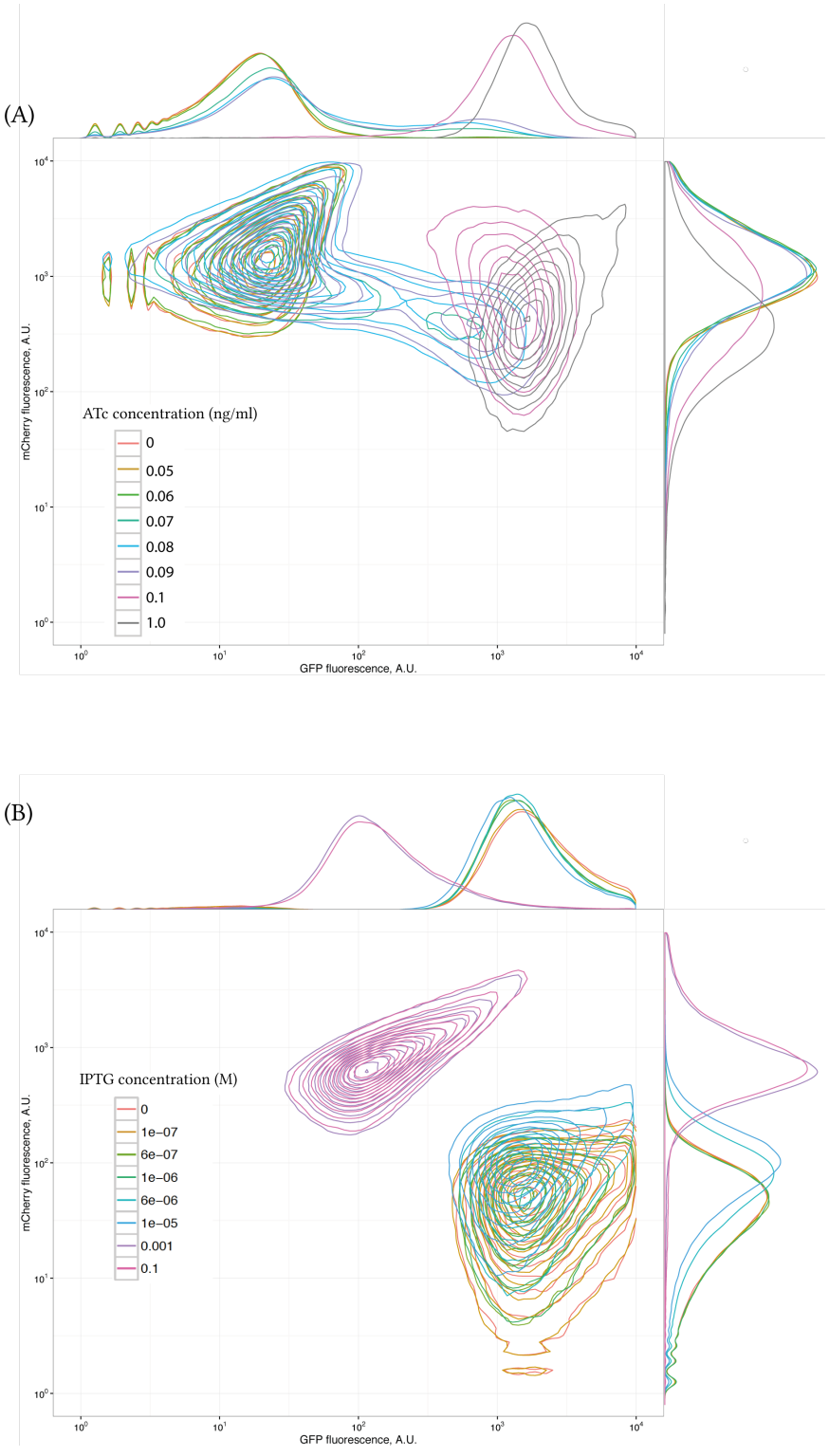

Figure 1.17 : (A) ATc induction at various concentrations (B) IPTG induction at various concentrations.

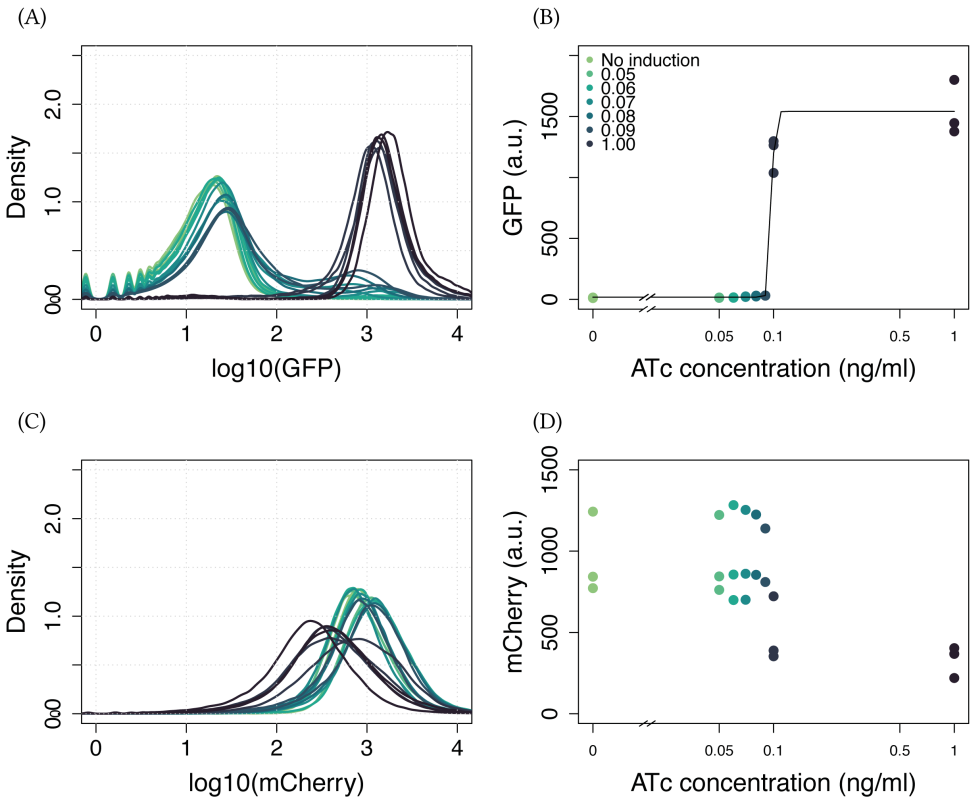

Figure 1.18 (A) Flow cytometry density plots of the logged GFP fluorescence obtained for each ATc induction. (B) There is an 84.1 fold increase in GFP fluorescence with increasing ATc concentration. (C) Flow cytometry density plots of the logged mCherry fluorescence obtained for each ATc induction. The medians of the flow cytometry densities of the triplicates of ATc induction. We observe a decrease in mCherry fluorescence.

model, in order to be able to fit the data collected. We observe a 84.1 fold increase in GFP fluorescence. We also observe a decrease in mCherry fluorescence during ATc induction. The dynamical range of GFP is larger than the dynamical range of mCherry during ATc induction.s

During IPTG induction we observe an increase in mCherry fluorescence, as seen in Figure 1.19. The parameters obtained via the nonlinear least squares estimation are $P_{min} = 7.3$, $P_{max} = 687.3$, $K_d = 0.00012$, and $n = 0.98$. There is a 94.5 fold increase in mCherry fluorescence. We also observe a decrease in GFP fluorescence with increasing IPTG concentrations.

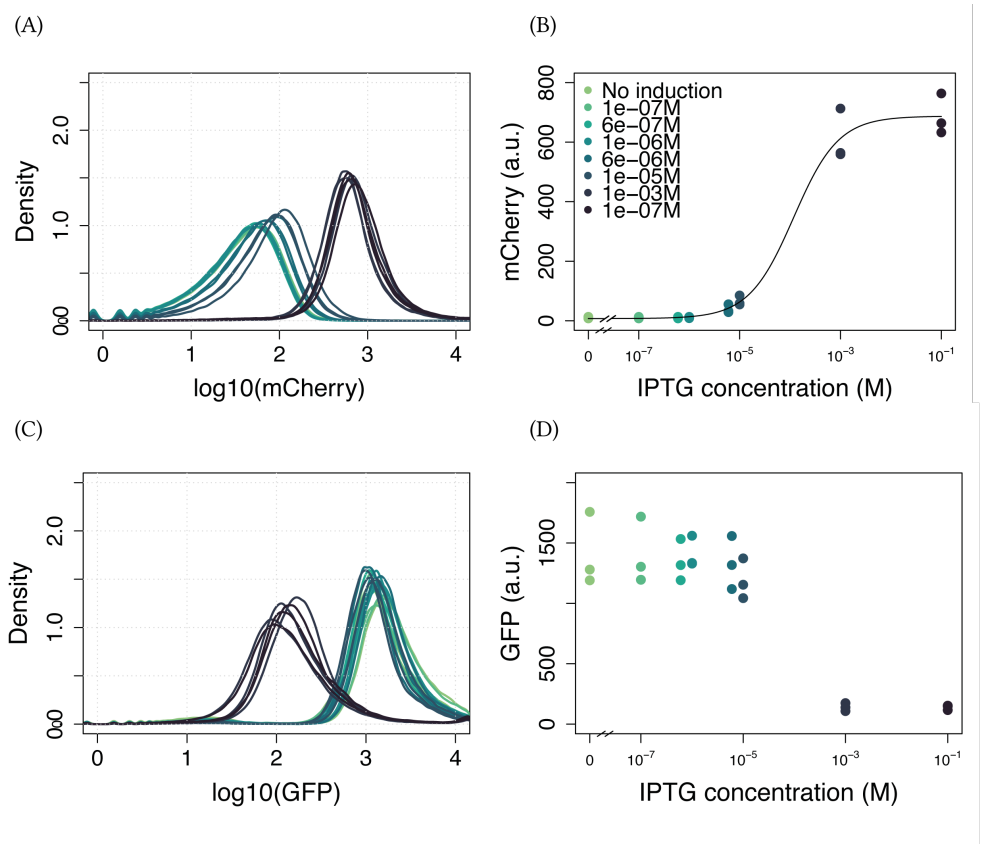

Figure 1.19 : (A) Flow cytometry density plots of the logged mCherry fluorescence obtained for each IPTG induction. (B) There is a 94.5 fold increase in mCherry fluorescence with increasing IPTG concentration. (C) Flow cytometry density plots of the logged GFP fluorescence obtained for each IPTG induction. The medians of the flow cytometry densities of the triplicates of IPTG induction. We observe a decrease in GFP fluorescence.

Figures 1.18 and 1.19 demonstrate that the genetic toggle switch present on the pKDL071 plasmid is capable of behaving like a switch. By adding the appropriate inducers at increasing concentrations I observed the switch flipping between its two states, GFP high/mCherry low and GFP low/mCherry high. I observed a bigger fold increase in fluorescence in mCherry during IPTG inductions compared to GFP during ATc inductions. Both inductions resulted in a large overall change in fluorescence for the two fluorescent proteins GFP and mCherry.

1.6.3.5 Toggle switch time course assay

I further analysed the pKDL071 toggle switch by investigating the time it takes for it to switch from one high state to the other. To do that I used the method outlined in Section 1.6.2.16. I obtained separate time courses for the IPTG and ATc inductions.

As can be seen in Figure 1.20 pKDL071 ATc induction begins switching 1 hour after induction. Complete induction is seen at 6 hours. During the IPTG induction (Figure 1.21) we see a bimodal distribution at 4 hours, and induction is complete at 6 hours. We observe that during ATc induction there is an increase in GFP fluorescence and a decrease in mCherry fluorescence, in the case of IPTG induction the increase in mCherry fluorescence is not as prominent. A decrease in GFP fluorescence is observed during IPTG induction.

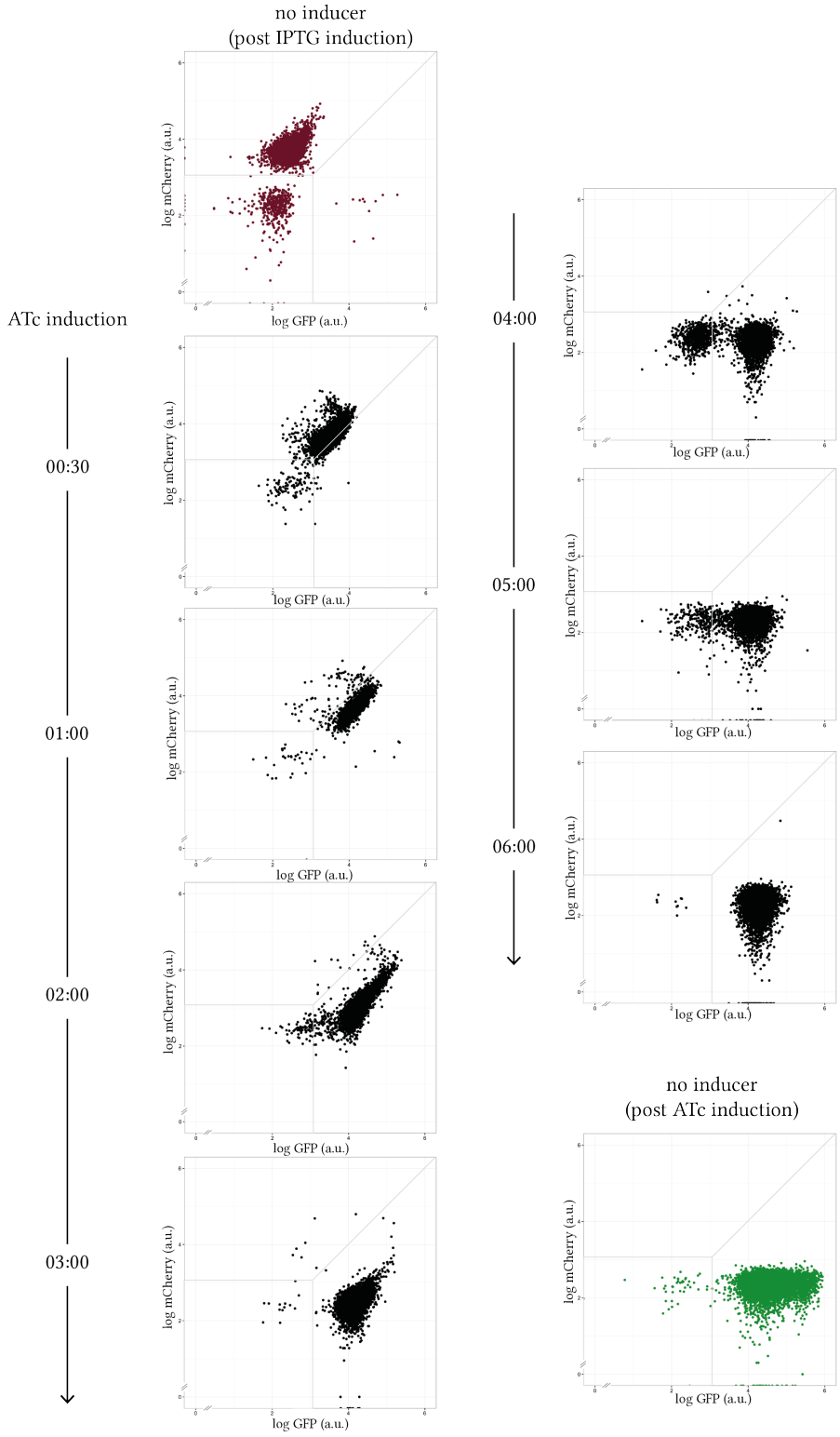

Figure 1.20 ATc induction of pKDL071 over time

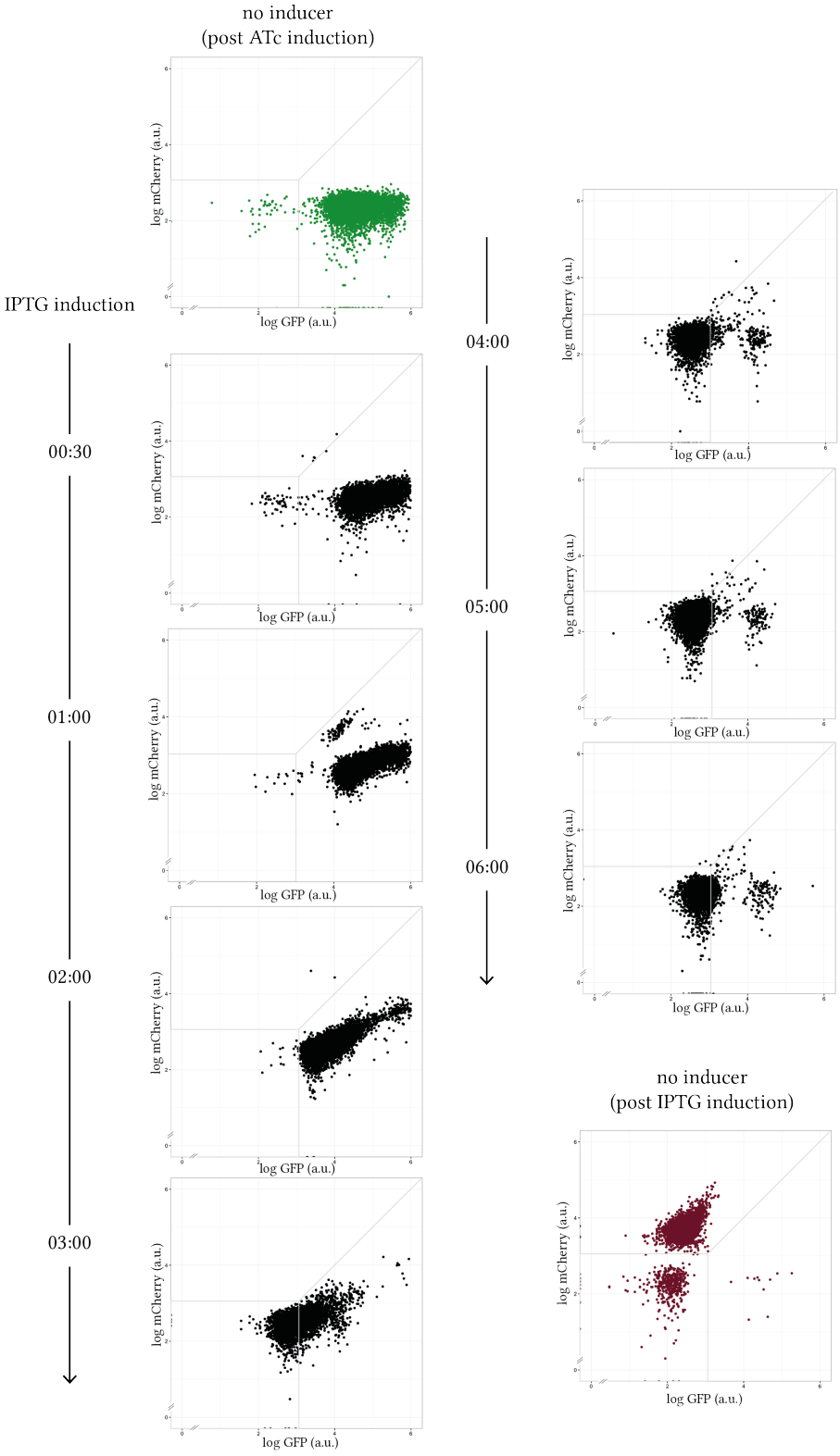

Figure 1.21 IPTG induction of pKDL071 over time

In the next section I use ABC-FLow to fit a computational model to the timecourse data obtained. Prior to fitting a model to it, I process the data by removing the unresponsive populations. This ensures that the model is fitted only to the data from cells that respond to the inducers. As seen in Figure 1.20, during the ATc induction there is an unresponsive population of cells where GFP and mChery fluorescence are both less that 10^3. This population is excluded from further analysis of the data. During the IPTG induction there is a population of cells that does not repsond to the addition of IPTG by switching from GFP high to mCherry high. This population of cells is also excluded from further analysis.

1.7 ABC-Flow used on experimental data

In this section I apply ABC-Flow to the experimental flow cytometry data collected in Section 1.6.3.5. The data set is comprised of time course data of the Litcofsky et al. (2012) toggle switch. The two states of the switch are represented by the levels of GFP and mCherry intensity in each bacterial cell. Using ATc inducer, each cell transitions from a mCherry high state to a GFP high state and using IPTG each cell transitions from a GFP high state to an mCherry high state.

1.7.1 Toggle switch model developed to fit to experimental data

The model used to fit the toggle switch time course assays was developed by using the Shea-Ackers formalism which represents the probability of a given promoter expressing (Ackers, Johnson, & Shea 1982). The Shea-Ackers formalism is described in Section ??. In order to take into account the stochastic dynamics of the system, the Gillespie algorithm is used in ABC-Flow, and thus the toggle switch model is described by the following hazards:

$$h_1 = KD_u(1 + KI_u)GFP \tag{1.9}$$

$$h_2 = 60\frac{R_u KL_u}{1 + KL_u + KR_u mCherry^2} \tag{1.10}$$

$$h_3 = KD_v(1 + KI_v)mCherry \tag{1.11}$$

$$h_4 = 60\frac{R_v KL_v}{1 + KL_v + KR_v GFP^2}, \tag{1.12}$$

where GFP and mCherry represent the two fluorescent proteins in the system. The cooperativity of the repressors is represented in the model. KI_u and KI_v KL_u KL_v

KD_u KD_v KR_u KR_v, parameters KI_u and KI_v increase the degradation of one of the species, and simulates the addition of a repressor, IPTG or ATc respectively. When using this model to fit to the post-ATc induction time course data, KI_v was set to 0. KI_u was set to 0, until t=0.01h where the prior distribution was used. This was done to simulate the addition of the inducer. When using this model to fit the post-IPTG induction time course, KI_u was set to 0 and KI_v sampled from the prior after t=0.01h.

The two production hazards, $h2$ and $h4$ are multiplied by 60 to reflect the copy number of the toggle switch plasmid in each cell. The plasmid containing the toggle switch used here, pKDL071, contains the ColE1 origin of replication, and thus 50-70 copies of the plasmid are present in each cell (Milo et al. 2010).

The priors used in ABC-Flow for this model are given in Table 1.10. All priors given assume a uniform ditribution. The values where chosen in agreement with (Lillacci & Khammash 2013) and in reference to http://bionumbers.hms.harvard.edu/, the database of useful biological numbers (Milo et al. 2010).

In order to account for background fluorescence I used the fluorescence level of the OFF states of the switch. After the overnight induction of the toggle switch with ATc and IPTG, the fluorescent intensity of the OFF state was considered to be the background fluorescence present. This was added to the model at each timepoint.

Table 1.10 The priors used for the 1D and 2D ABC-FLow model fitting to flow cytometry data

Parameters				
Description	Symbol	Units	ATc induction	IPTG induction
IPTG-induced mCherry degradation rate	KI_u	h^{-1} μM^{-1}		1 - 10
GFP transcription rate	R_u	molecules h^{-1}	1 - 50	1 - 50
GFP translation rate	KL_u	h^{-1}	1 - 50	1 - 50
GFP degradation	KD_u	h^{-1}	0.1 - 2	0.1 - 2
mCherry-induced GFP repression rate	KR_u	molecules^{-1} h^{-1}	0.016 - 1.2	0.016 - 1.2
mCherry transcription rate	R_v	molecules h^{-1}	1 - 50	1 - 50
mCherry translation rate	KL_v	h^{-1}	1 - 50	1 - 50
GFP-induced mCherry repression rate	KR_v	molecules^{-1} h^{-1}	0.016 - 1.2	0.016 - 1.2
mCherry degradation	KD_v	h^{-1}	0.1 - 2	0.1 - 2
ATC-induced GFP degradation rate	KI_v	h^{-1} μM^{-1}	1 - 10	
Species				
	GFP	mM	0 - 1	100 - 1000
	mCherry	mM	100 - 1000	0 - 1
Intensity paramters				
Mean of fluorescence of single GFP molecule	μ_{GFP}	AU	5 - 200	5 - 200
Mean of fluorescence of single mCherry molecule	$\mu_{mCherry}$	AU	5 - 200	5 - 200
Standard deviation of fluorescence of single GFP molecule	σ_{GFP}	AU	5 - 200	5 - 200
Standard deviation of fluorescence of single mCherry molecule	$\sigma_{mCherry}$	AU	5 - 200	5 - 200

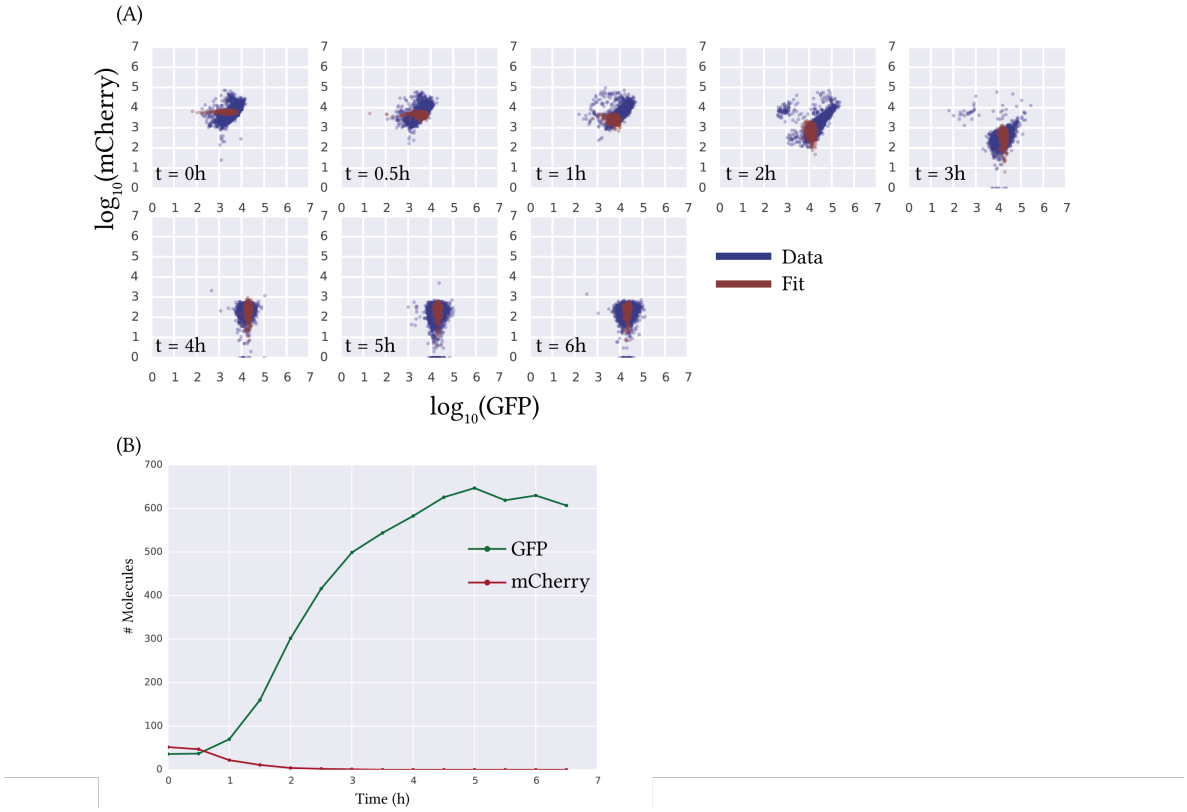

Figure 1.22 (A) The post-ATc induction flow cytometry timecourse data (blue) and the resulting model fit from ABC-Flow (red). (B) The model simulation using parameters sampled form the posterior distribution shows that this model behaves like a switch.

1.7.2 Model fitting to the genetic toggle switch post ATc induction

I first use ABC-Flow to fit the model described in Section 1.7.1 o the post-ATc induction timecourse of the toggle switch. I used the data set obtained in Section 1.6.2.16. The data was pre-processed by removing the population of cells that were unresponsive to the inducer. The prior distribution used is given in Table 1.10. ABC-Flow returned the posterior distributions of the parameters that could reproduce the experimental data. The posterior distributions are given in Figure 1.25.

Figure 1.22 shows the resulting time course data of the model using parameters sampled from the posterior distribution. The model was also simulated without converting the number of molecules to fluorescence intensity in order to confirm that the model behaves like a switch. This is shown in Figure 1.22B. We confirm that this model, using parameters sampled from the posterior distribution obtained

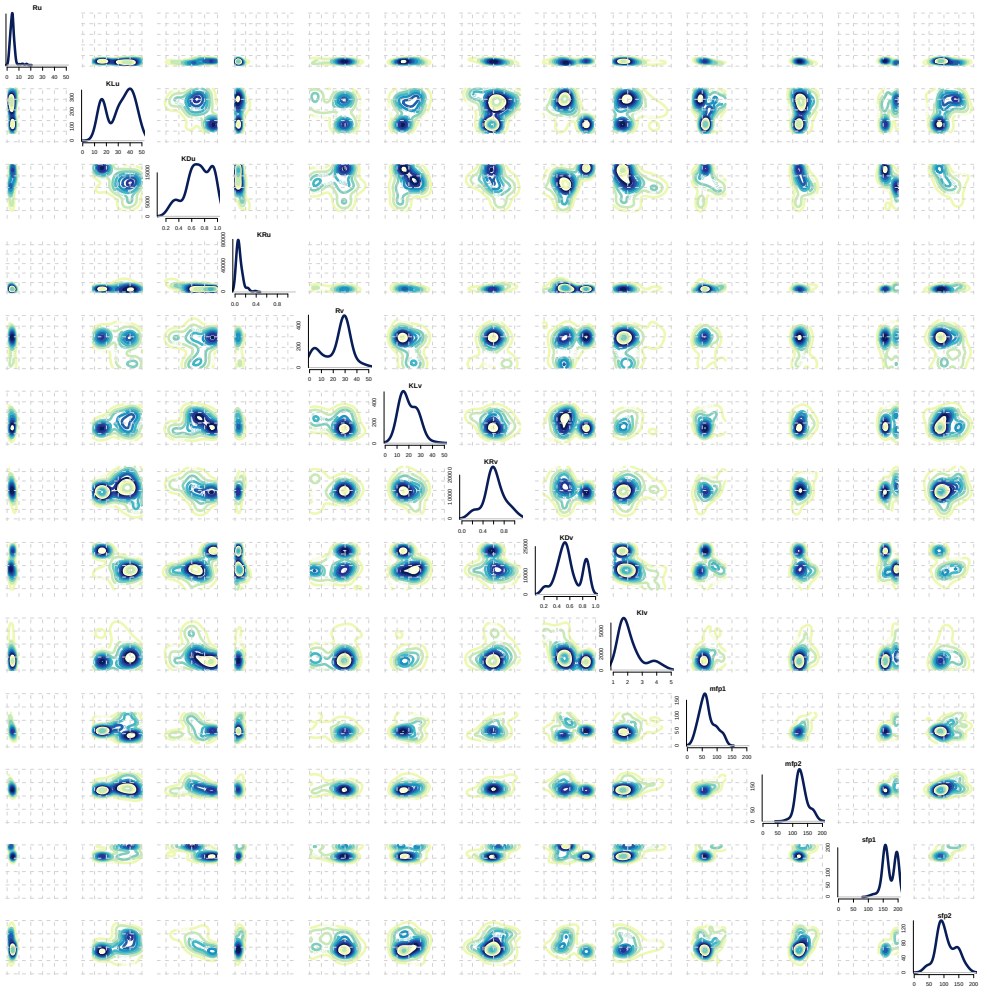

Figure 1.23 The posterior distributions of the 13 parameters fitted to post-ATC induction time course data using ABC-Flow. We find that the paramters for GFP expression (R_u) and repression (KR_u) are the most constrained.

from ABC-Flow behaves like a switch. Following ATC-induction, the number of GFP molecules increases and the number of mCherry molecules decreases.

The posterior distribution obtained form ABC-Flow is shown in Figure 1.25. We find that the parameter for GFP gene expression, R_u must be low, whereas there are no constraints on the values of gene expression for mCherry. The parameter for the repression of GFP by mCherry is also constrained to be low.

1.7.3 Model fitting to the genetic toggle switch post IPTG induction

In this section I use ABC-Flow to fit the experimental time course obtained from the toggle switch post-IPTG induction. The prior densities used are given in Table 1.10. The resulting time course of the model fitted to the experimental flow cytometry data is shown in Figure 1.24.

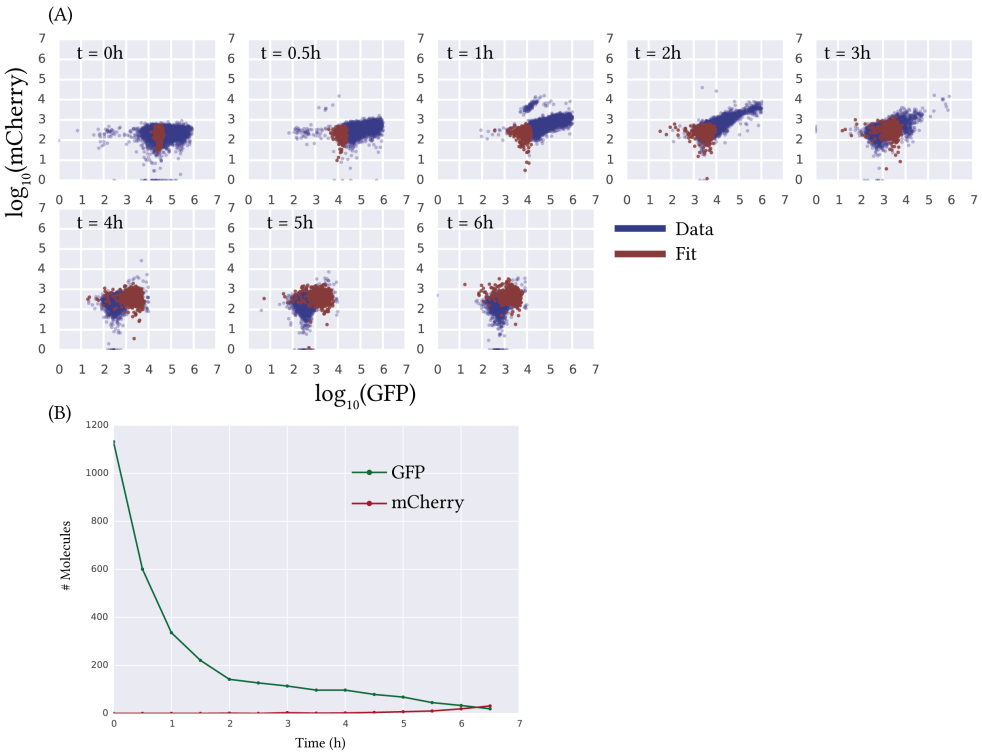

Figure 1.24 (A) The time course data obtained of the post-IPTG induced toggle switch is shown in blue and the resulting fit from ABC-Flow is shown in red. (B) The model was simulated by using parameter sampled from the posterior distribution. The resulting model did not behave like a switch.

As can be seen in Figure 1.24B, the toggle switch model simulated using the parameters fitted to the post-IPTG timecourse data does not behave like a switch within the timeframe given from the experimental data (0-6 hours). We find a rapid decay of GFP without an increase in mCherry fluorescence as would be expected. This could be attributed to the experimental timecourse obtained. As shown in Figure 1.24A, over a period of 6 hours post induction there is a decrease in GFP fluorescence. mCherry can be seen increasing after two hours post indution but

then not maintaining that high level. Over the 6 hours, there is no overall increase in mCherry fluorescence. This timecourse would be challenging to fit using the model used here as it does not behave like a switch as expected.

The posterior density obtained from by ABC-Flow is given in Figure 1.25. we find parameter R_u, representing GFP expression, to be very constrained to be low. We also find the parameters representing the mean of the normal distribution sampled for the conversion of number of GFP molecules to intensity to be constrained.

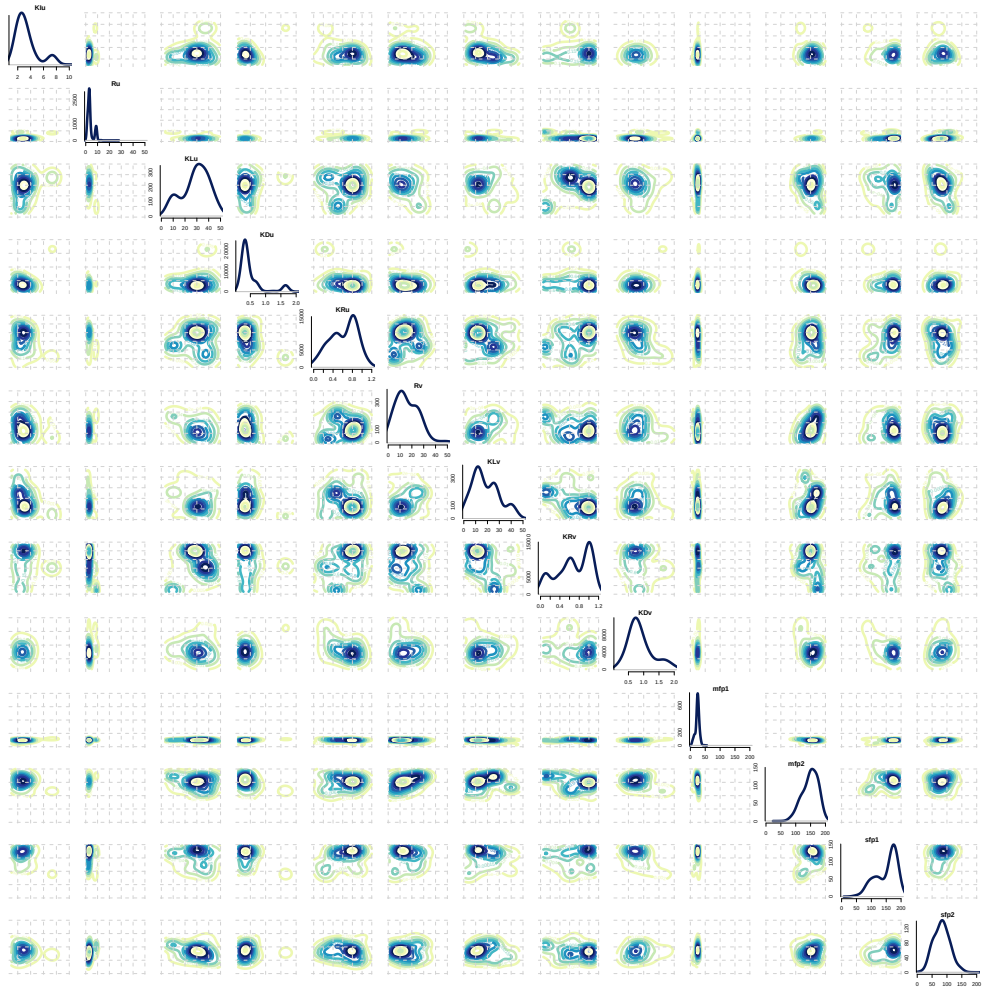

Figure 1.25 The posterior distribution obtained from ABC-Flow for the post-IPTG timecourse data. The parameter for GFP expression was found to be the most constrained.

The final epsilon used in both switch inductions was set to 10. This is a sufficient distance in order to obtain a distribution that is close to the experimental data set, as shown in Section 1.4.2. Nevertheless, given that the data set does not represent a

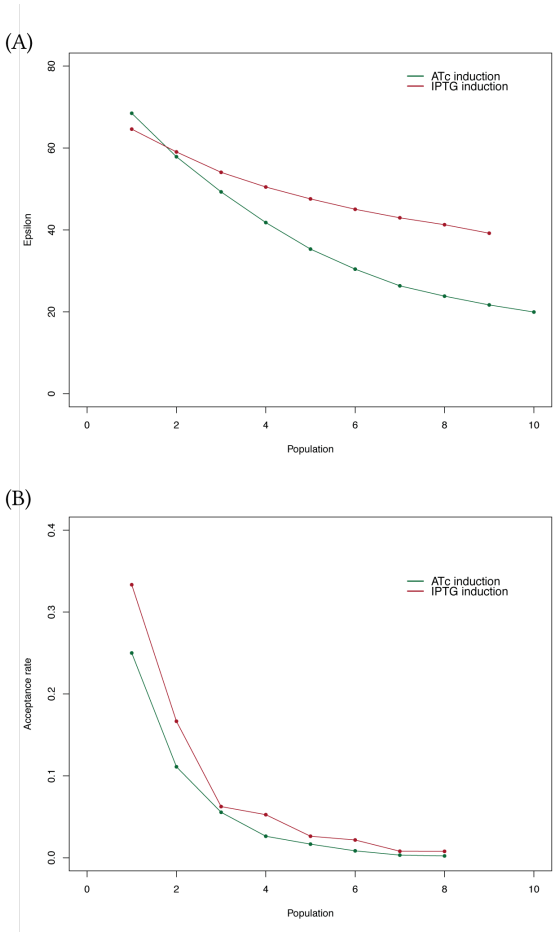

Figure 1.26 (A) The progression of epsilons over the populations in ABC-Flow for ATc (green) and IPTG (red) induction. (B) The acceptance rate decreases rapidly with every population.

normal distribution, it was not possible to obtain a fit with such a low epsilon value. The populations were allowed to progress until the reduction in epsilon started to plateaux and the acceptance rate becomes very low. This indicates that the fit will not improve significantly with subsequent populations. The progression of the epsilons and the acceptance rates are given in Figure 1.26. The epsilon progression of the fit for the IPTG induction of the switch further confirms that the fit to the data is not very good. Epsilon reduction levels off at a high epsilon value compared to the ATc induction, while the acceptance rate is very low. This indicates that continuing with the fit of the above model to the IPTG induction data will not produce a better fit.

In this section I used ABC-Flow to fit a toggle switch model to experimental flow

cytometry data. Both sides of the switch were examined, ATc induction which flips the switch from mCherry high to GFP high and IPTG induction, which flips the switch from GFP high to mCherry high. The model was successfully fit to the data set obtained from the ATc induction of the switch but less so to the data obtained from the IPTG induction of the switch.

1.8 Discussion

Here I developed a Bayesian framework, ABC-Flow, that is used to fit stochastic models to flow cytometry data. Fitting computational models to flow cytometry data can be challenging; fluorescence intensity is measured in arbitrary units (a.u.) and there can be a big variability between experiments depending on instrument settings. This poses a challenge for model fitting as the fluorescence intensity emitted by each individual fluorophore molecule cannot be reliably estimated (Kelwick et al. 2014). ABC-Flow converts the number of molecules obtained via simulations to fluorescence intensity in order to overcome current limitations in fitting computational models to flow cytometry data. The novelty of this framework is that it can be used on two-dimensional flow cytometry data simultaneously.

Here I have used ABC-Flow to fit the toggle switch model to simulated flow cytometry data in one and two dimensions. This demonstrated the effectiveness of ABC-Flow in parameter identifiability. ABC-Flow is an extension to the method proposed by Lillacci & Khammash (2013), referred to as *INSIGHT*, but can be used on two dimensional flow cytometry data. This makes it ideal to be used on the genetic toggle switch, whose behaviour is reflected by the levels of two fluorescent proteins, GFP and mCherry.

I used ABC-Flow to fit a stochastic computational model to flow cytometry time course data obtained by inducing the genetic toggle switch to its two states. This was done using both sides of the switch, GFP high/mCherry low to GFP low/mCherry high and vice versa. A good fit was obtained for the ATc induction, representing the flip from GFP low to GFP high. The fit was not as good for the other side of the switch, obtained via IPTG induction. This could be attributed to the experimental data obtained. Post-IPTG induction we observed a decrease in GFP but the increase in mCherry was not as prominent. This result could be improved by a repetition of the time course experiment, which was not carried out due to time constraints.

Both fits could be improved by a number of methods in the future. Firstly, the flow cytometry data can be calibrated in order to account for instrument and set-

tings variability. This can be done by using commercially available calibration beads. Computational methods like FlowCal, developed by Tabor et al. (2009) can be used to convert fluorescence arbitrary units (a.u.) to MEFs (molecules of equivalent fluorophore). This can account for instrument gain settings as well as day to day instrument variability. Future improvements on ABC-Flow would also include the simultaneous fitting of the toggle switch model to both timecourses, post ATc and post IPTG induction. Both of these timecourses are obtained from the same genetic system, and the accurate characterisation of said system would have to include both functions. This would allow us to obtain parameter estimates for components that can respond to both inducers. ABC-Flow could be also be further developed to be able to fit computational models to more fluorophores simultaneously. This would enable the effective characterisation of more complex systems.

In this Chapter I also characterised the genetic toggle switch experimentally. First I study the effect of the two inducers ATc and IPTG on the growth rate of the selected chassis *E. coli* K-12 MG1655. I find that there is no detrimental effect to the bacterium by the inducers. I further characterised the switch by determining the minimum inducer concentration necessary to change the state of the switch. I find that for ATc induction, a minimum of $0.09\,\mathrm{ng\,mL^{-1}}$ is required to cause the switch to go to a GFP high state. For IPTG induction I find that a minimum of 0.001 M is required to flip the switch to an mCherry high state. This information is critical for using this switch in other applications. Both sides of the switch are very sensitive to inducer concentrations, as the concentrations required to observe a change in fluorescence are very small.

Furthermore I find that this toggle switch, pKDL071, is faster to respond to a change in ATc concentration that to a change in IPTG concentration. For IPTG induction we observe a change in fluorescence after 3-4 hours of induction. For ATc induction we can see a difference within an hour of induction. This result is in agreement with Litcofsky et al. (2012). This difference in response times must be taken into account when using the pKDL071 switch for other applications. This difference could be due to maturation times of the fluorescent proteins. Macdonald, Chen, & Mueller (2012) found that mCherry half-maturation time is 150 mins, whereas the GFP variant used here, GFPmut3b has been especially mutated for fast action (Cormack, Valdivia, & Falkow 1996). Cormack, Valdivia, & Falkow (1996) found that whereas wild type GFP is detectable 1-2 hours after induction, GFPmut3b is detectable 8 minutes after induction. This difference could account for the different response times observed. This difference is also observed in the fitted computational

models of the system. The computational model used here to fit these timecourse data did not account for fluorophore maturation time, as a summary parameter of GFP production was used instead. A more detailed model could be used to further investigate this difference. Since ABC-Flow simulates the models in order to obtain the posterior density, the size of the model will not be an obstacle in parameter estimation.

The use of computational models is crucial to understand the complex processes underlying observed biological phenomena (Lillacci & Khammash 2013). This has proved especially important in the advancement of synthetic biology, which strives to produce systems with well-defined functions (Chin 2006) and reliable operation (Lu, Khalil, & Collins 2009). Being able to have a well-parameterised model of a synthetic gene network can aid in the reliable use of such system. It can also aid in the further design and improvement of the synthetic system. Further modifications to the synthetic gene network can be tested *in silico*.

Furthermore, several competing constructs can be compared for their robustness to parameter fluctuations. An advantage of ABC-Flow is that it uses a Bayesian framework, which can estimate ranges of parameter values that can produce a behaviour rather. Competing genetic systems can be compared for their volume of the parameter ranges that can produce their observed behaviour. A small parameter range suggests that a small fluctuation in parameter values will cause the genetic system to not behave as expected, which would render it undesirable for a real-world application.

1.9 Summary

In this chapter I developed ABC-Flow, a Bayesian framework used to fit computational models to flow cytometry data. I tested the method using simulated data. I summarised the experiments carried out for the analysis of the genetic toggle switch. I used the pKDL071 plasmid and characterised its switching behaviour over various inducer concentrations and over time. I found the concentration of each inducer necessary to flip the switch as well as the time it takes for the change to be observed. The timecourse experiments were used as input to ABC-FLow in order to fit a computational model to the data. In the next Chapter I outline an experimental design to construct more robust genetic toggle switches.

Bibliography

Ackers, G. K., Johnson, A. D., & Shea, M. A. (1982). 'Quantitative model for gene regulation by lambda phage repressor.' *Proceedings of the National Academy of Sciences of the United States of America* **79**(4), 1129–1133.

Bower, A. G., McClintock, M. K., & Fong, S. S. (2010). 'Synthetic biology: a foundation for multi-scale molecular biology.' *Bioengineered Bugs* **1**(5), 309–312.

Chin, J. W. (2006). 'Programming and engineering biological networks'. *Current Opinion in Structural Biology* **16**(4), 551–556.

Choi, S.-L., Rha, E., Lee, S. J., Kim, H., Kwon, K., Jeong, Y.-S., Rhee, Y. H., Song, J. J., Kim, H.-S., & Lee, S.-G. (2014). 'Toward a generalized and high-throughput enzyme screening system based on artificial genetic circuits.' *ACS Synthetic Biology* **3**(3), 163–171.

Cooling, M. T., Rouilly, V., Misirli, G., Lawson, J., Yu, T., Hallinan, J., & Wipat, A. (2010). 'Standard virtual biological parts: a repository of modular modeling components for synthetic biology.' **26**(7), 925–931.

Cormack, B. P., Valdivia, R. H., & Falkow, S. (1996). 'FACS-optimized mutants of the green fluorescent protein (GFP)'. *Gene* **173**(1), 33–38.

Díaz, M., Herrero, M., García, L. A., & Quirós, C. (2010). 'Application of flow cytometry to industrial microbial bioprocesses'. *Biochemical Engineering Journal* **48**(3), 385–407.

Ellis, B., Gentleman, R., Hahne, F., Le Meur, N., Sarkar, D., & Jiang, M. (2016a). *flowViz: Visualization for flow cytometry*. R package version 1.36.2.

Ellis, B., Haaland, P., Hahne, F., Le Meur, N., Gopalakrishnan, N., Spidlen, J., & Jiang, M. (2016b). *flowCore: flowCore: Basic structures for flow cytometry data*. R package version 1.38.2.

Fasano, G. & Franceschini, A. (1987). 'A multidimensional version of the Kolmogorov-Smirnov test'. *Monthly Notices of the Royal Astronomical Society* **225**(1), 155–170.

Fedorec, A. J. (2016). *autoGate*. https://github.com/ajfedorec/autoGate.git.

Friedman, J. H. & Rafsky, L. C. (1979). 'Multivariate generalizations of the Wald-Wolfowitz and Smirnov two-sample tests'. *The Annals of Statistics*.

Gardner, T. S., Cantor, C. R., & Collins, J. J. (2000). 'Construction of a genetic toggle switch in Escherichia coli'. *Nature* **403**(6767), 339–342.

Gillespie, D. T. (1977). 'Exact Stochastic Simulation of Coupled Chemical-Reactions'. *Journal of Physical Chemistry* **81**(25), 2340–2361.

Kelly, J. R., Rubin, A. J., Davis, J. H., Ajo-Franklin, C. M., Cumbers, J., Czar, M. J., de Mora, K., Glieberman, A. L., Monie, D. D., & Endy, D. (2009). 'Measuring the activity of BioBrick promoters using an in vivo reference standard.' *Journal of Biological Engineering* **3**(1), 4–4.

Kelwick, R., MacDonald, J. T., Webb, A. J., & Freemont, P. (2014). 'Developments in the tools and methodologies of synthetic biology.' *Frontiers in bioengineering and biotechnology* **2**, 60–60.

Kolmogorov, A. N. (1933). 'Sulla Determinazione Empirica di Una Legge di Distribuzione'. *Giornale dell'Istituto Italiano degli Attuari* **4**, 83–91.

Lillacci, G. & Khammash, M. (2013). 'The signal within the noise: efficient inference of stochastic gene regulation models using fluorescence histograms and stochastic simulations.' *Bioinformatics (Oxford, England)* **29**(18), 2311–2319.

Litcofsky, K. D., Afeyan, R. B., Krom, R. J., Khalil, A. S., & Collins, J. J. (2012). 'Iterative plug-and-play methodology for constructing and modifying synthetic gene networks.' *Nature Methods* **9**(11), 1077–1080.

Lopes, R. H. C., Reid, I., & Hobson, P. R. (2007). 'The two-dimensional Kolmogorov-Smirnov test'. In: *International Workshop on Advanced Computing and Analysis Techniques in Physics Research*. Amsterdam, 1–12.

Lu, T. K., Khalil, A. S., & Collins, J. J. (2009). 'Next-generation synthetic gene networks'. *Nature Biotechnology* **27**(12), 1139–1150.

Lutz, R. & Bujard, H. (1997). 'Independent and tight regulation of transcriptional units in Escherichia coli via the LacR/O, the TetR/O and AraC/I1-I2 regulatory elements.' *Nucleic Acids Research* **25**(6), 1203–1210.

Macdonald, P. J., Chen, Y., & Mueller, J. D. (2012). 'Chromophore maturation and fluorescence fluctuation spectroscopy of fluorescent proteins in a cell-free expression system.' *Analytical Biochemistry* **421**(1), 291–298.

Major, S. (2016). *ndtest*. https://github.com/syrte/ndtest.git.

Milo, R., Jorgensen, P., Moran, U., Weber, G., & Springer, M. (2010). 'BioNumbers–the database of key numbers in molecular and cell biology.' *Nucleic Acids Research* **38**(Database issue), D750–D753.

Monaco, J. V. (2014). 'Classification and Authentication of One-dimensional Behavioral Biometrics'. In: *International Journal of Cognitive Biometrics*, 1–8.

Shaner, N. C., Campbell, R. E., Steinbach, P. A., Giepmans, B. N. G., Palmer, A. E., & Tsien, R. Y. (2004). 'Improved monomeric red, orange and yellow fluorescent proteins derived from Discosoma sp. red fluorescent protein.' *Nature Biotechnology* **22**(12), 1567–1572.

Shapiro, H. M. (1941). *Practical flow cytometry*. Wiley-Liss.

Shimomura, O., Johnson, F. H., & Saiga, Y. (1962). 'Extraction, purification and properties of aequorin, a bioluminescent protein from the luminous hydromedusan, Aequorea.' *Journal of Cellular and Comparative Physiology* **59**, 223–239.

Tabor, J. J., Salis, H. M., Simpson, Z. B., Chevalier, A. A., Levskaya, A., Marcotte, E. M., Voigt, C. A., & Ellington, A. D. (2009). 'A Synthetic Genetic Edge Detection Program'. *Cell* **137**(7), 1272–1281.

Team, R. D. C. (2008). *R: A language and environment for statistical computing*. R Foundation for Statistical Computing. ISBN: 3-900051-07-0. URL: www.Rproject.org.

Wald, A. & Wolfowitz, J. (1940). 'On a test whether two samples are from the same population'. *The Annals of Mathematical Statistics*.

Wickham, H. (2009). *ggplot2: Elegant Graphics for Data Analysis*. Springer-Verlag New York. ISBN: 978-0-387-98140-6. URL: http://ggplot2.org.

Wilk, M. B. & Gnanadesikan, R. (1968). 'Probability plotting methods for the analysis of data.' *Biometrika* **55**(1), 1–17.